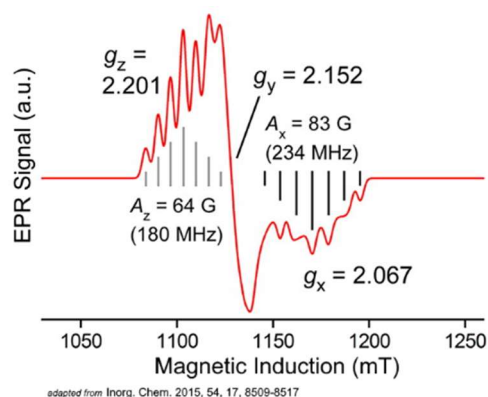# C312: Electron Spin Resonance of Doublet and Triplet Copper Paramagnets

Length of Practical: 12 Hours, in pairs

Pre-Requisites

- 2nd Year Quantum Option
- S217 Computational NMR Spectroscopy
- S218 An introduction to Python for Chemists
- Recommended to those of keen Physical Chemistry interest

$g_z = 2.201$

$g_y = 2.152$

$A_x = 83$ G (234 MHz)

$A_z = 64$ G (180 MHz)

$g_x = 2.067$

*adapted from Inorg. Chem. 2015, 54, 17, 8509-8517*

Objectives

- To explore g-anisotropy and construction of the powder ESR spectrum.
- To introduce the effects of molecular rotational rates on the ESR spectra.
- To determine the nature of the copper-ligand bond in terms of covalency via applications of ligand field theory.
- To gain experience in the practical aspects of ESR data acquisition and analysis.

Introduction

This practical introduces basic considerations for ESR simulations, measurements, and data analysis of two Cu(II) molecules: tetraphenylporphyrinatocopper(II) has one unpaired electron and tetra-μ_2-acetatodiaquadicopper(II) has two unpaired electrons that have strong exchange coupling. The only known naturally occurring copper porphyrin molecules are found in the bright red tail feathers of the African touraco bird (Musophagidae). Copper acetate has been used as a shark repellant, in electroplating, and as a starting material for CuO nanoparticles.
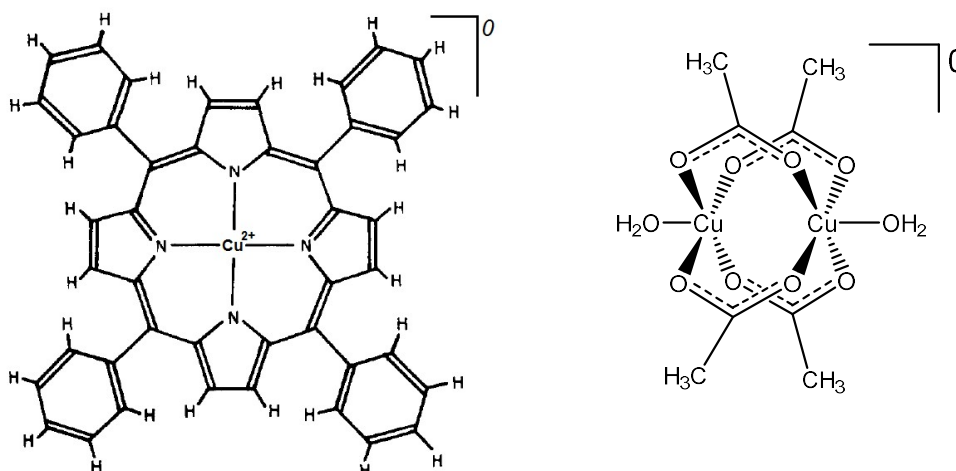
Scheme 1. Left is tetraphenylporphyrinatocopper(II), CuTPP, which is S=1/2 and right, tetra-μ_2-acetatodiaquadicopper(II), a.k.a. copper acetate, which is two anti-ferromagnetic coupled spin ½ ions that results in S = 0 ground state and S = 1 excited state, separated by exchange coupling.

NMR and ESR have many similarities, e.g. $h\nu = g\mu_B B$ for ESR and $h\nu = g\mu_N B$ for NMR. Here h is Planck's constant, ν is the Larmor frequency, g is the electron or nuclear g-factor, μ_B is the Bohr magneton, μ_N is the nuclear magneton, and B is the magnetic flux density, or magnetic induction, given in units of Tesla. For electrons the spin moment has the opposite sense as the magnetic moment, unlike in ^{1}H-NMR. As result, the electron-Zeeman interaction results in negative spin values being lower in energy. For example, S = 1/2 spin systems have m_s = -1/2 lower than m_s = 1/2. These are also commonly referred to as β and α spin states, respectively. The g-values that are useful for this lab are below.
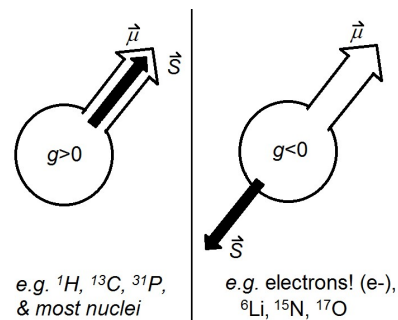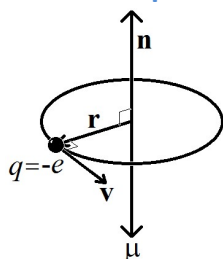
e.g. ^{1}H, ^{13}C, ^{31}P, & most nuclei

e.g. electrons! (e-), ^{6}Li, ^{15}N, ^{17}O

Table 1.	Natural Abundance	spin	g-value	gyromagnetic ratio [10^7 rad s^{-1} T^{-1}]
e$^-$	1.0	1/2	-2.0023193	17608.597
^{1}H	0.999885	1/2	5.58569468	26.75222
^{14}N	0.99636	1	0.403761	1.9337798
^{63}Cu	0.6915	3/2	1.484897	7.111791
^{65}Cu	0.3085	3/2	1.5877	7.6043

Orbital & Spin Angular momentum and derivation of resonant transition energy
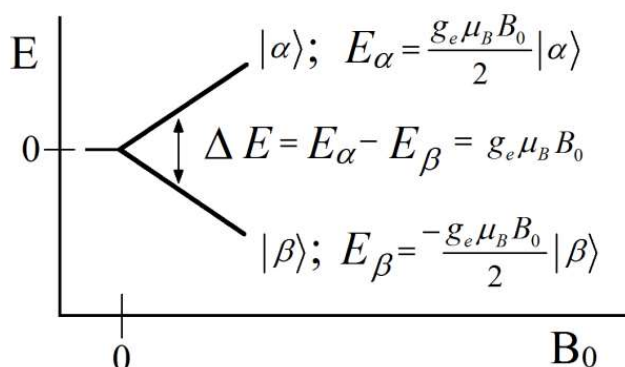
For an electron moving in circle, the magnetic moment is given as $\boldsymbol{\mu}=I A\mathbf{n}$, where I is the current and A is the area of the circle. Consider that $I=q/T$, where q is the charge of an electron ($-e$) and T is revolution time ($2\pi r/v$). The magnetic moment is then $\boldsymbol{\mu} = (-ev/2\pi r)(\pi r^2)\mathbf{n} = (-evr/2)\mathbf{n}$. You may know angular momentum defined as the cross product of position with respect to the origin about which it rotates and momentum ($\boldsymbol{l} = \boldsymbol{r} \times \boldsymbol{p}$), with $p = m_e v$, the mass of the electron times its velocity. Thus the angular momentum can be re-written as $\boldsymbol{l} = r m_e v\mathbf{n}$, and using $rv\mathbf{n} = \boldsymbol{l}/m_e$, we have $\boldsymbol{\mu} = (-e/2m_e)\boldsymbol{l}$ (see Dirac §35 for a more general description). With the Bohr magneton, $\mu_B=(-e\hbar/2m_e)$, $\boldsymbol{\mu} = \mu_B \boldsymbol{l}/\hbar$.

The eigenvectors of angular momentum are spherical harmonics of Y_{lm}, with $l = \{0,1,2,...\}$ and $m = \{-l,-l+1,...l\}$ (often given as Y_{kq} in ESR), where the total angular moment $\hat{L}^2\left|lm\right\rangle = l(l+1)\mathrm{h}^2\left|lm\right\rangle$ and the state of the system is given by $\hat{L}_z\left|lm\right\rangle = m\mathrm{h}\left|lm\right\rangle$, not $\left\langle lm\right|\hat{L}_x\left|lm\right\rangle = \left\langle lm\right|\hat{L}_y\left|lm\right\rangle = 0$. In contrast, $\hat{L}_x$ and $\hat{L}_y$ change the state of system, following the ladder operators $\hat{L}_+ = \hat{L}_x + i\hat{L}_y$ and $\hat{L}_- = \hat{L}_x - i\hat{L}_y$: $\hat{L}_\pm|l,m_l\rangle = \sqrt{l(l+1) - m_l(m_l \pm 1)}\hbar|l,m_l \pm 1\rangle$. For a single electron $l=S=\frac{1}{2}$, so $m_s =\{-\frac{1}{2}, \frac{1}{2}\}$. For the magnetic field directed along the z direction: $\hat{H} = -\mu \cdot B = \dfrac{g_e\mu_B}{\mathrm{h}}\left(\hat{S}_x,\hat{S}_y,\hat{S}_z\right)\begin{pmatrix}0\\0\\B_0\end{pmatrix} = \dfrac{g_e\mu_B B_0 \hat{S}_z}{\mathrm{h}}$.

Given eigenstates for the electron of m_s = ½ = $\left|\alpha\right\rangle$ and m_s = -½ = $\left|\beta\right\rangle$,

$\hat{H}\left|\alpha\right\rangle = \dfrac{g_e\mu_B B_0}{\mathrm{h}}\hat{S}_z\left|\alpha\right\rangle = \dfrac{g_e\mu_B B_0}{2}\left|\alpha\right\rangle$ and

$\hat{H}\left|\beta\right\rangle = \dfrac{g_e\mu_B B_0}{\mathrm{h}}\hat{S}_z\left|\beta\right\rangle = \dfrac{-g_e\mu_B B_0}{2}\left|\beta\right\rangle$, we can

draw the Zeeman effect for the transition energy as a function of increasing magnetic field, shown to the right → :

$\left|\alpha\right\rangle; \ E_\alpha = \dfrac{g_e\mu_B B_0}{2}\left|\alpha\right\rangle$

$\Delta E = E_\alpha - E_\beta = g_e\mu_B B_0$

$\left|\beta\right\rangle; \ E_\beta = \dfrac{-g_e\mu_B B_0}{2}\left|\beta\right\rangle$

Spin System Operators

Recall the Pauli spin matrices (problem 12.7 in Atkins & dePaula, Physical Chemistry, 8th ed.; Dirac §37):

$$\sigma_x = \begin{pmatrix} 0 & 1 \\ 1 & 0 \end{pmatrix} \quad \sigma_y = \begin{pmatrix} 0 & -i \\ i & 0 \end{pmatrix} \quad \sigma_z = \begin{pmatrix} 1 & 0 \\ 0 & -1 \end{pmatrix} \quad \sigma_0 = \begin{pmatrix} 1 & 0 \\ 0 & 1 \end{pmatrix}$$

The matrix σ_0 is also called the unit operator or just **1**. To obtain the basic spin operators for an $S=1/2$ molecule these matrices are multiplied by one-half times hbar.
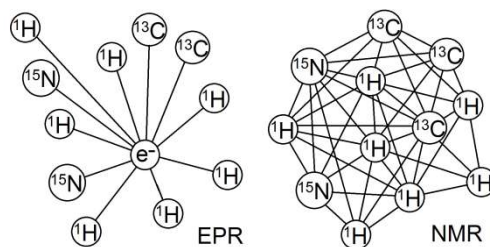
$$\hat{S}_x = \hbar \begin{pmatrix} 0 & \frac{1}{2} \\ \frac{1}{2} & 0 \end{pmatrix} \quad \hat{S}_y = \hbar \begin{pmatrix} 0 & -i/2 \\ i/2 & 0 \end{pmatrix} \quad \hat{S}_z = \hbar \begin{pmatrix} \frac{1}{2} & 0 \\ 0 & -\frac{1}{2} \end{pmatrix} \quad \hat{S}_+ = \hbar \begin{pmatrix} 0 & \frac{1}{2} \\ 0 & 0 \end{pmatrix} \quad \hat{S}_- = \hbar \begin{pmatrix} 0 & 0 \\ \frac{1}{2} & 0 \end{pmatrix}$$

In the case of $S = 1/2$, these operate as

	$\hat{S}_x$	$\hat{S}_y$	$\hat{S}_z$
$\lvert\alpha\rangle$	$\frac{1}{2}\lvert\beta\rangle$	$\frac{1}{2}i\lvert\beta\rangle$	$\frac{1}{2}\lvert\alpha\rangle$
$\lvert\beta\rangle$	$\frac{1}{2}\lvert\alpha\rangle$	$-\frac{1}{2}i\lvert\alpha\rangle$	$-\frac{1}{2}\lvert\beta\rangle$

For this practical, you may be interested the matrices for $I = 1$ (^{14}N) and $I = 3/2$ ($^{63/65}$Cu), which are included in Appendix A. ESR is fundamentally different from NMR in that the spin systems approximately follow the pictorial comparison to the right. In the case of an electron spin distributed over many nuclei, the ESR measurement is only the sum of individual electron-nuclear pair interactions, not between nuclear spins. To form the overall spin operator of the spin system in the case of one proton ($I = \frac{1}{2}$) and one electron ($S = \frac{1}{2}$), one would need to redefine the spin operators in the total dimension of known as Hilbert space by calculating a direct product (a.k.a. Kronecker product or outer product). Here is the corresponding spin operator for the electron in such a spin system of a proton and electron.

$$\hat{S}_x = \hat{s}_x \otimes \mathbf{1} = \begin{pmatrix} 0 & \frac{1}{2} \\ \frac{1}{2} & 0 \end{pmatrix} \otimes \begin{pmatrix} 1 & 0 \\ 0 & 1 \end{pmatrix} = \begin{pmatrix} 0 & 0 & \frac{1}{2} & 0 \\ 0 & 0 & 0 & \frac{1}{2} \\ \frac{1}{2} & 0 & 0 & 0 \\ 0 & \frac{1}{2} & 0 & 0 \end{pmatrix}.$$

Note that the matrix is 4 x 4 and its basis vector contains $N = 4$ values [*Exercise*, give an appropriate basis vector ___ ___ ___ ___]. The basis vector for N spins of a single spin value is given as $(2S+1)^N$, while multiple types of spin values ($S_a=3/2$, $S_b=6$, $S_c=7/2$, etc.) have dimensions of $(2S_a+1)^{Na} (2S_b+1)^{Nb}(2S_c+1)^{Nc}...$, where the total basis is formed from the direct product of all spins considered in the system. The examples of this practical are CuTPP and copper acetate. If we limit CuTPP to only considering the electron, $^{63/65}$Cu, and the first coordination sphere, ^{14}N, the Hilbert space dimension is $(2(1/2)+1)(2(3/2)+1)(2(1)+1)^4 = 648$ or 648 x 648 elements. For copper acetate the only significant spins are the electrons and copper nuclei, or $(2(1)+1)(2(3/2)+1)^2 = 48$. Hilbert space calculations are sufficient for CW-ESR measurements focused on describing the time-independent Hamiltonian of a spin system. For consideration of relaxation dynamics, pulsed ESR, slow-motion and kinetics one would expand the basis to Liouville space with dimensions of $(2S+1)^N$ x $(2S+1)^N$ for N spins of a single value. This is an advanced topic covered Trinity term magnetic resonance (*P. Hore*).

ESR Spin Hamiltonian

The transition frequencies and transition probabilities of ESR derive from the spin Hamiltonian. For electron k, neighboring electron m, and nucleus i, a description of the spin Hamiltonian is as follows:

$$H = \sum_m J_{mk}\bar{S}_m\bar{S}_k + \{\bar{S}_k\tilde{D}_{km}\bar{S}_k\} + \mu_B\bar{S}_k\tilde{g}\vec{B}_0$$

$$+ \sum_i \bar{S}_k\tilde{A}_i\bar{I}_i - \sum_i \mu_N g_N B_0 \bar{I}_{zi} + \sum_i \bar{I}_{zi}\tilde{Q}_i\bar{I}_{zi} + \sum_m \bar{S}_k\tilde{D}_{km}\bar{S}_m + \bar{S}\tilde{C}\bar{J}$$

These terms are ordered according to their typical magnitude: exchange, fine structure splitting or zero-field splitting (ZFS), electron Zeeman interaction, hyperfine interaction (HFC), nuclear Zeeman interaction, nuclear quadrupole interaction (QPI), electron-electron dipolar interaction, and finally, spin rotation.

The form of these interaction tensors are as follows (*pre-factors omitted*), similar to the Dot Product:

Linear (Zeeman) $\begin{bmatrix} \hat{S}_x & \hat{S}_y & \hat{S}_z \end{bmatrix} \begin{bmatrix} g_{xx} & g_{yx} & g_{zx} \\ g_{xy} & g_{yy} & g_{zy} \\ g_{xz} & g_{yz} & g_{zz} \end{bmatrix} \begin{bmatrix} \vec{B}_x \\ \vec{B}_y \\ \vec{B}_z \end{bmatrix} = g_{xx}\hat{S}_x\vec{B}_x + g_{yx}\hat{S}_y\vec{B}_x + \cdots$

Bilinear (HFC) $\begin{bmatrix} \hat{S}_x & \hat{S}_y & \hat{S}_z \end{bmatrix} \begin{bmatrix} A_{xx} & A_{yx} & A_{zx} \\ A_{xy} & A_{yy} & A_{zy} \\ A_{xz} & A_{yz} & A_{zz} \end{bmatrix} \begin{bmatrix} \hat{I}_x \\ \hat{I}_y \\ \hat{I}_z \end{bmatrix} = A_{xx}\hat{S}_x\hat{I}_x + A_{yx}\hat{S}_y\hat{I}_x + \cdots$

Quadratic (ZFS, QPI) $\begin{bmatrix} \hat{S}_x & \hat{S}_y & \hat{S}_z \end{bmatrix} \begin{bmatrix} D_{xx} & D_{yx} & D_{zx} \\ D_{xy} & D_{yy} & D_{zy} \\ D_{xz} & D_{yz} & D_{zz} \end{bmatrix} \begin{bmatrix} \hat{S}_x \\ \hat{S}_y \\ \hat{S}_z \end{bmatrix} = D_{xx}\hat{S}_x^2 + D_{yx}\hat{S}_y\hat{S}_x + \cdots$

The Cartesian spin operators $\begin{bmatrix} \hat{S}_x & \hat{S}_y & \hat{S}_z \end{bmatrix}$ & $\begin{bmatrix} \hat{I}_x & \hat{I}_y & \hat{I}_z \end{bmatrix}$ define the *eigenbasis* and as discussed on page 6-3, may contain 10s to > 1000s of matrix elements. Next, calculation of *eigenvalues* and *eigenvectors* is performed to characterize the energy level splittings of the spin system. The orientation of the molecule is accounted for by the rotation of the interaction tensors with respect to the magnetic field. A sufficient number of orientations of the molecule with respect to the magnetic field allows calculation of the powder pattern of the ESR spectrum. Such a set of orientations is shown on the right. Each interaction tensor of the spin Hamiltonian may be *rotated* into its <u>principle axis</u>, yielding three <u>principle values</u> on the diagonal, such as gx, gy, and gz.
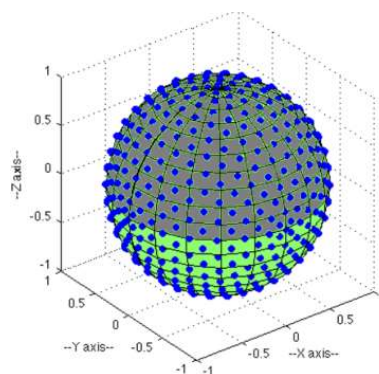
Electron Zeeman Interaction $\hat{H}_{EZ} = \mu_B \bar{S}_k g \bar{B}_0$

For an isotropic spin or a single orientation of a molecule the electron Zeeman interaction is $\hat{H} = \omega\hat{S}_z$, where ω is the precession frequency in radians per second of the electron, $\omega = -\gamma B_0$.

g-shift

In NMR you have seen that a *shift* in the resonance position of signals, following $\hat{H}_{NZ} = -\gamma(1-\sigma)B_0\hat{I}_Z$, where the overall shift is $\sigma = \sigma_p^{local} + \sigma_d^{local} + \sigma_N + \sigma_R + \sigma_e + \sigma_i$ (*see 3rd yr NMR notes of C.R. Timmel*). In ESR there are similar shifts to the g-value such that its observed, or effective, value is diagnostic of several contributions:

$g_{eff} = g_e^{(free)} + g^{RMC} + g^{GC} + g^{SOC/OZ}$, with $\hat{H}_{EZ} = \mu_B g_{eff} B_0\hat{S}_Z$. The first is the term, g_e, is that of the free electron and some physicists study it exclusively, (with) *Q.E.D.* A relativistic mass correction, g^{RMC}, is applied due to the orbital effects. Then there is a gauge correction, g^{gc}, concerning the location of the g-tensor

within the molecule (usually placed in the center of electron density). Finally, there is the spin-orbit coupling term, which has the largest contribution for transition metals, and may also include an orbit-Zeeman component if orbital angular momentum is unquenched. One may calculate the contribution for spin-orbit coupling via the Landé g-factor, and a more extensive discussion with respect to anisotropy is below.

$$g_J = 1 + \frac{j(j+1) + s(s+1) - l(l+1)}{2j(j+1)}.$$

Anisotropy in the g-tensor

While isotropic chemical shift values are usually found in solution state NMR, the chemical shift *anisotropy* (CSA) in solid state NMR is analogous to g-value anisotropy of solid state ESR as both are linear tensor interactions. In NMR it is $\hat{H}_{NZ} = -g_N \mu_N \hat{I} \cdot B_0 = -g_N \mu_N (\hat{I}_x, \hat{I}_y, \hat{I}_z) \cdot (1-\boldsymbol{\sigma}) \cdot \bar{B}_0$, or in the full matrix:

$$\hat{H}_{NZ} = -g_N \mu_N (\hat{I}_x, \hat{I}_y, \hat{I}_z) \cdot \begin{pmatrix} 1-\sigma_{xx} & \sigma_{xy} & \sigma_{xz} \\ \sigma_{yx} & 1-\sigma_{yy} & \sigma_{yz} \\ \sigma_{zx} & \sigma_{zy} & 1-\sigma_{zz} \end{pmatrix} \cdot \begin{pmatrix} B_{0x} \\ B_{0y} \\ B_{0z} \end{pmatrix}$$

For a disordered sample of fixed orientations, we can use polar coordinates, $[B_x\ B_y\ B_z] = B_0 * [n_x\ n_y\ n_z]$, where direction cosines are $n_x = \sin\theta\cos\varphi$, $n_y = \sin\theta\sin\varphi$, and $n_z = \cos\theta$. The anisotropic electron Zeeman interaction is as follows.

$$\hat{H}_{EZ} = \mu_B B_0 (\hat{S}_x, \hat{S}_y, \hat{S}_z) \cdot \begin{pmatrix} g_{xx} & g_{xy} & g_{xz} \\ g_{yx} & g_{yy} & g_{yz} \\ g_{zx} & g_{zy} & g_{zz} \end{pmatrix} \cdot \begin{pmatrix} n_x \\ n_y \\ n_z \end{pmatrix}$$

For a simple $S=1/2$, with $|\alpha\rangle, |\beta\rangle$ basis, this may be written in a matrix form as

$$\hat{H}_{EZ} = \mu_B B_0 \begin{bmatrix} \dfrac{n_z g_{zz}}{2} & \dfrac{n_x g_{xx}}{2} - \dfrac{i n_y g_{yy}}{2} \\ \dfrac{n_x g_{xx}}{2} + \dfrac{i n_y g_{yy}}{2} & \dfrac{-n_z g_{zz}}{2} \end{bmatrix}$$

By solving the secular equation (determinant), the effective g-value is found as [*challenge: do it yourself*]

$$g_{eff}^2 = g_x^2 \cos^2\varphi \sin^2\theta + g_y^2 \sin^2\varphi \sin^2\theta + g_z^2 \cos^2\theta$$

Effective g-value

Isotropic, axial, or orthorhombic? _____

What are the limiting g-value(s)? ___ , ___ , ___

In the blue box are plots of effective g-values showing the dependence B_0 field orientation for a highly anisotropic low-spin ferric haem.
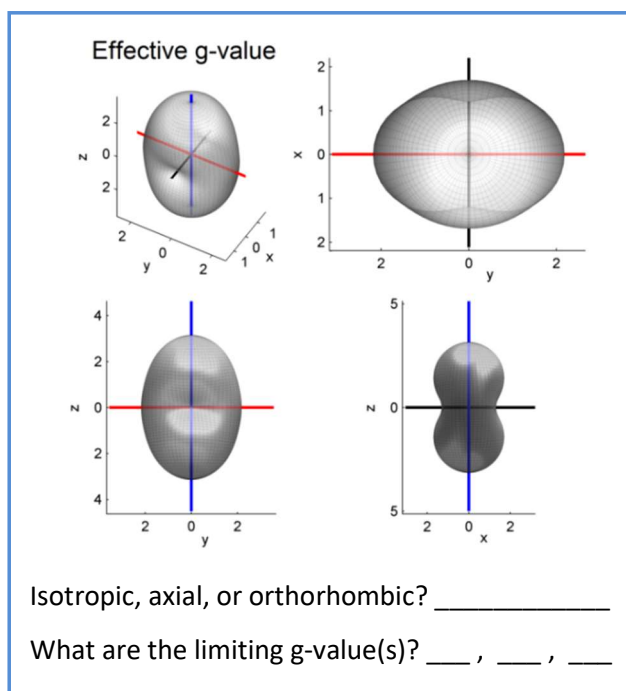
g-tensor Categories:
isotropic $\qquad g_x = g_y = g_z$
axial $\qquad g_x = g_y \neq g_z$ or $g_x \neq g_y = g_z$
orthorhombic $\qquad g_x \neq g_y \neq g_z$

You will explore these g-value tensors shapes on Day 1.

For an axial g-tensor the effective g-value reduces to $\qquad g_{eff}^2 = g_\perp^2 \sin^2\theta + g_P^2 \cos^2\theta$.

Spin-orbit interaction as a source of g-matrix anisotropy

The spin-orbit interaction is most often responsible for the anisotropy of the g-tensor, noting orbital contributions of different nuclei proportional to Z^4 (Se > S > O). The electron Zeeman interaction becomes

$$\hat{H}_{EZ} = -\mu_e \cdot \overline{B}_0 = \mu_B \overline{B}_0 \left(\hat{L} + g_e \hat{S} \right) + \zeta \hat{L} \cdot \hat{S}$$

For an electron in a p-orbital, $\left| p_x \right\rangle = \dfrac{-1}{\sqrt{2}}\left(\left|1,1\right\rangle - \left|1,-1\right\rangle \right), \left| p_y \right\rangle = \dfrac{i}{\sqrt{2}}\left(\left|1,1\right\rangle - \left|1,-1\right\rangle \right), \left| p_z \right\rangle = \dfrac{i}{\sqrt{2}}\left(\left|1,0\right\rangle \right)$ with a

basis of $\left| l, m \right\rangle$. The angular momentum operators l_x, l_y, and l_z for the p and d orbitals, operate as follows:

Table 2.	l_x	l_y	l_z
$\|p_x\rangle \equiv \|x\rangle$	0	$-i\|z\rangle$	$i\|y\rangle$
$\|p_y\rangle \equiv \|y\rangle$	$i\|z\rangle$	0	$-i\|x\rangle$
$\|p_z\rangle \equiv \|z\rangle$	$-i\|y\rangle$	$i\|x\rangle$	0
$\|d_{x2-y2}\rangle \equiv \|x^2-y^2\rangle$	$-i\|yz\rangle$	$-i\|xz\rangle$	$2i\|xy\rangle$
$\|d_{z2}\rangle \equiv \|z^2\rangle$	$-i\sqrt{3}\|yz\rangle$	$i\sqrt{3}\|xz\rangle$	0
$\|d_{xy}\rangle \equiv \|xy\rangle$	$i\|xz\rangle$	$-i\|yz\rangle$	$-2i\|x^2-y^2\rangle$
$\|d_{xz}\rangle \equiv \|xz\rangle$	$-i\|xy\rangle$	$i\|x^2-y^2\rangle-i\sqrt{3}\|z^2\rangle$	$i\|yz\rangle$
$\|d_{yz}\rangle \equiv \|yz\rangle$	$i\|x^2-y^2\rangle+i\sqrt{3}\|z^2\rangle$	$i\|xy\rangle$	$-i\|xz\rangle$

$\hat{\mathcal{H}}_{SO} = \zeta \hat{L} \cdot \hat{S}$ is for p-orbitals:

Table 3.	$\|x,\alpha\rangle$	$\|y,\alpha\rangle$	$\|z,\alpha\rangle$	$\|x,\beta\rangle$	$\|y,\beta\rangle$	$\|z,\beta\rangle$
$\langle x,\alpha\|$	0	$-i/2$	0	0	0	$1/2$
$\langle y,\alpha\|$	$i/2$	0	0	0	0	$-i/2$
$\langle z,\alpha\|$	0	0	0	$-1/2$	$i/2$	0
$\langle x,\beta\|$	0	0	$-1/2$	0	$i/2$	0
$\langle y,\beta\|$	0	0	$-i/2$	$-i/2$	0	0
$\langle z,\beta\|$	$1/2$	$i/2$	0	0	0	0

and for d-orbitals (↓):

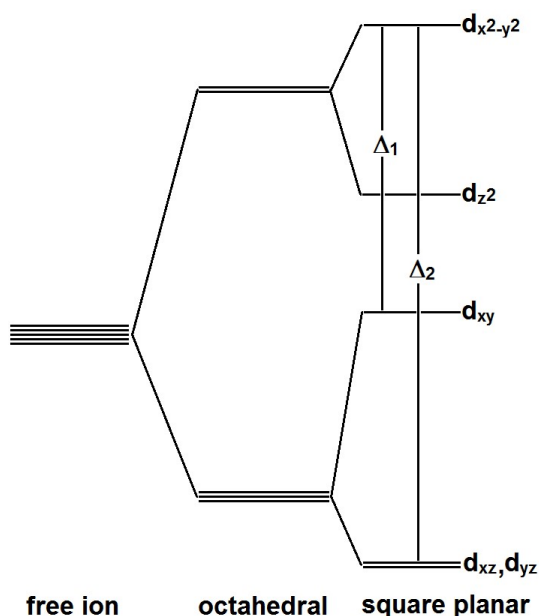| Table 4.	$\|x^2-y^2,\alpha\rangle$	$\|xy,\alpha\rangle$	$\|yz,\alpha\rangle$	$\|xz,\alpha\rangle$	$\|z^2,\alpha\rangle$	$\|x^2-y^2,\beta\rangle$	$\|xy,\beta\rangle$	$\|yz,\beta\rangle$	$\|xz,\beta\rangle$	$\|z^2,\beta\rangle$
$\langle x^2-y^2,\alpha\|$	0	$-i$	0	0	0	0	0	$+i/2$	$+1/2$	0
$\langle xy,\alpha\|$	$+i$	0	0	0	0	0	0	$+1/2$	$-i/2$	0
$\langle yz,\alpha\|$	0	0	0	$+i/2$	0	$-i/2$	$-1/2$	0	0	$-i\sqrt{3}/2$
$\langle xz,\alpha\|$	0	0	$-i/2$	0	0	$-1/2$	$+i/2$	0	0	$+\sqrt{3}/2$
$\langle z^2,\alpha\|$	0	0	0	0	0	0	0	$+i\sqrt{3}/2$	$-\sqrt{3}/2$	0
$\langle x^2-y^2,\beta\|$	0	0	$+i/2$	$-1/2$	0	0	$+i$	0	0	0
$\langle xy,\beta\|$	0	0	$-1/2$	$-i/2$	0	$-i$	0	0	0	0
$\langle yz,\beta\|$	$-i/2$	$+1/2$	0	0	$-i\sqrt{3}/2$	0	0	0	$-i/2$	0
$\langle xz,\beta\|$	$+1/2$	$+i/2$	0	0	$-\sqrt{3}/2$	0	0	$+i/2$	0	0
$\langle z^2,\beta\|$	0	0	$+i\sqrt{3}/2$	$+\sqrt{3}/2$	0	0	0	0	0	0

Magic Pentagon
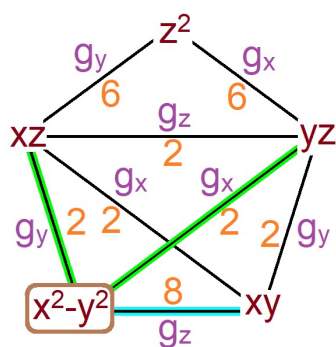
$\dfrac{m_L}{0}$ ... ±1 ... ±2

For the d-orbitals of transition metal it is conventional to use the *magic pentagon* to determine coefficients from the spin orbit coupling, as is shown in *Appendix A.2*. Application of the spin-orbit coupling of Cartesian d-orbitals makes use of their definitions in ($|L, m_L\rangle$):

$$\left| d_{z^2} \right\rangle = \left|2,0\right\rangle,$$

$$\left| d_{xz} \right\rangle = \frac{-1}{\sqrt{2}}\left(\left|2,1\right\rangle - \left|2,-1\right\rangle \right), \left| d_{yz} \right\rangle = \frac{i}{\sqrt{2}}\left(\left|2,1\right\rangle + \left|2,-1\right\rangle \right)$$

$$\left| d_{x^2-y^2} \right\rangle = \frac{1}{\sqrt{2}}\left(\left|2,2\right\rangle + \left|2,-2\right\rangle \right), \left| d_{xy} \right\rangle = \frac{-i}{\sqrt{2}}\left(\left|2,2\right\rangle - \left|2,-2\right\rangle \right)$$

free ion   octahedral   square planar

Mixing of excited states in spin-orbit interaction

In the case of CuTPP, the Cu(II) free ion is ^2D with $^2T_{2g}$ orbitals of O_h split in **D_{4h}** to $^2B_{2g}$ (d_{xy}) above and ^2E_g (d_{xz}, d_{yz}) below. The ^2E_g state of O_h symmetry splits in D_{4h} tetragonal elongation to $^2B_{1g}$ (d_{x2-y2}) above and below, $^2A_{1g}$ (d_{z2}). By looking at the character tables, one will see that spin rotation along the z-axis (Rz) <u>mixes *excited states*</u> of x^2-y^2 (b1g) and xy (b2g) involving a promotion of an electron from the lower *d*-orbital to d_{x2-y2}. Thus we have a spin-orbit contribution about the z-axis seen in the <u>magic pentagon</u> with **$n = 8$** following the **cyan line** along bottom of the pentagon or by multiplying the D_{4h} point group irreducible representations B_{1g} (x^2-y^2) * A_{2g} (**Rz**) = B_{2g} (direct product of symmetry comp.):

$$g_z = g_e - \frac{a^2 n\lambda}{E_{x^2-y^2} - E_{xy}}$$

An equation for the g-value represented by rotation in the x-axis and y-axis based on <u>pentagon</u> with **$n = 2$** following either **green line** from the x^2-y^2 point to xz or yz of the pentagon or by multiplying the D_{4h} point group irreducible representations B_{1g} (x^2-y^2) * E_g (**$R_{x,y}$**) = E_g:

$$g_x = g_y = g_e - \frac{a^2 n\lambda}{E_{x^2-y^2} - E_{xz,yz}}$$

Here the spin orbit coupling is $\lambda = \pm\zeta/2S$ with the free ion value of $\zeta = -830\text{cm}^{-1}$ for copper. The covalency of the ligand is accounted for with value a^2 ($a^2 = 1$ is fully ionic) which is further developed in <u>post-lab question Q1c</u>. These g-value equations may employ doublet states described as $|\Psi^+\rangle \ and \ |\Psi^-\rangle$, composed of other spin orbitals ($|m_l,m_s\rangle$). Extensive unquenched orbital angular momentum and non-canonical coordination (mix of *d*-orbital character) may lead additional terms and computational approaches.

D_{4h}	E	$2C_4$ (z)	C_2	$2C'_2$	$2C''_2$	i	$2S_4$	σ_h	$2\sigma_v$	$2\sigma_d$	linear, **R**otations	quadratic	cubic
A_{1g}	+1	+1	+1	+1	+1	+1	+1	+1	+1	+1	-	x^2+y^2, z^2	-
A_{2g}	+1	+1	+1	-1	-1	+1	+1	+1	-1	-1	**Rz**	-	-
B_{1g}	+1	-1	+1	+1	-1	+1	-1	+1	+1	-1	-	x^2-y^2 x^2-y^2	-
B_{2g}	+1	-1	+1	-1	+1	+1	-1	+1	-1	+1	-	xy	-
E_g	+2	0	-2	0	0	+2	0	-2	0	0	(**R_x, R_y**)	(xz, yz)	-
A_{1u}	+1	+1	+1	+1	+1	-1	-1	-1	-1	-1	-	-	-
A_{2u}	+1	+1	+1	-1	-1	-1	-1	-1	+1	+1	z	-	z^3, $z(x^2+y^2)$
B_{1u}	+1	-1	+1	+1	-1	-1	+1	-1	-1	+1	-	-	xyz
B_{2u}	+1	-1	+1	-1	+1	-1	+1	-1	+1	-1	-	-	$z(x^2-y^2)$
E_u	+2	0	-2	0	0	-2	0	+2	0	0	(x, y)	-	(xz^2, yz^2) (xy^2, x^2y), (x^3, y^3)

The electron precession frequency is dependent on the total magnetic field, and the spins of surrounding nuclei contribute to the total field due to their magnetic moments. Thus the sum and difference of the local hyperfine field(s) and main magnetic field results in a splitting, called a hyperfine interaction. The spatial distribution for the hyperfine coupling of a nucleus with the unpaired electron is called an *A*-tensor. An example of several *A*-tensors of an organic radical is shown to the right, with proportional ellipsoids plotted at the location of the nucleus positions. With the relation of the g-tensor and *A*-tensors to the molecular frame, the structure of unknown paramagnetic molecules may be determined.
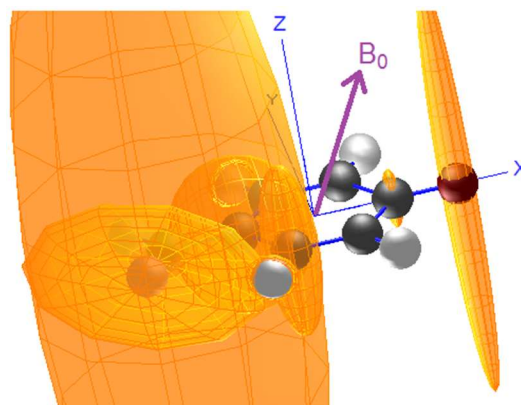
Selected *A*-tensor ellipsoids for 4-oxidobenzyl radical

The full hyperfine term is partitioned between through-space (dipolar) components and nuclear overlap (contact) components. For an axial hyperfine, $\overline{A} = a + \left[-T, -T, 2T\right]$, where *a* is the isotropic hyperfine and *T* is the dipolar component. The three elements, [-T, -T, 2T], represent the diagonal of the 3x3 hyperfine matrix. An orthorhombic hyperfine tensor may be parameterized by rhombicity, δ, such that the expression is $\overline{A} = a + T\left[-(1-\delta), -(1+\delta), 2\right]$. As in g-values, hyperfines are measured as *effective* values. The intrinsic hyperfine is $A_{int} = g_e * A_{eff}/g_{eff}$. Likewise, comparison of hyperfine values for metal centers of different spin value should be scaled by 1/2S. For organic radicals of $g \sim g_e$, the hyperfine couplings are often reported in Gauss. However the common unit is MHz. The conversion of Gauss to MHz is 1 G = 2.8 MHz.

Dipolar Hyperfine Interaction

The dipolar hyperfine of ligand nuclei and the paramagnetic electrons is almost always too weak to observe in CW-ESR and it requires high-resolution, advanced techniques such as Electron-Nuclear Double Resonance (ENDOR) and Electron Spin Echo Envelope Modulation (ESEEM), which are not covered in this practical. The anisotropic component of the hyperfine tensor, *T*, is given in its simplest form as a single point-dipole for the electron and nucleus distance, with respect to the magnetic field:

$$T = \frac{\mu_0}{4\pi h} \frac{g_e \mu_B g_n \mu_N}{r^3}, A_{dip} = T(3\cos^2\theta - 1)$$

The total hyperfine is then the sum of A_{iso} and A_{dip}, with θ defining the DC magnetic field and electron-nucleus vector. A convenient relation for ^{1}H nuclei is $A_{dip} = (1/r^3)*(3\cos^2\theta - 1)*79$ MHz.

Isotropic Hyperfine Interaction

In the fast-tumbling regime of an ESR sample, only the isotropic, or average, hyperfine coupling is defined in the ESR spectrum. The most basic formula for the hyperfine interaction is then $H_{HF} = aI \cdot S$. These strongly coupled nuclei split the ESR resonances of the electron according to Pascal triangle for identical hyperfine couplings, according to the rule 2nI+1, where n is the number of nuclei coupling to the electron and I is the nuclear spin number.

Fermi-Contact in hyperfine couplings is dependent on the amount of spatial overlap of the unpaired electron(s) and the nucleus. An equation for the hyperfine coupling of one electron in the s-orbital of a nucleus is below, with $|\Psi_o|^2$ being the spin density at the nucleus and ρ as the fraction of an electron and 1811 MHz being the isotropic hyperfine for a complete electron in an s-orbital of ^{14}N:

$$A_{iso} = \frac{2\mu_0}{3h} g_e \mu_B g_n \mu_N \rho |\Psi_0|^2, = \rho(1811 \text{ MHz})$$

A more extensive analysis of isotropic ^{14}N is possible isotropic hyperfine, where the contributions to of a full electron in 2s and 2p are considered separately. They differ by a factor 33, given the negligible overlap of the

2p orbital (Hartree, *et al.*, 1948). An extensive analysis of haem ^{14}N hyperfine has been used to make arguments about the hybridization of ^{14}N, e.g. for sp[2], $\rho(2s)=2*\rho(2p)$ (Scholes, *et al.*, 1982).

Zero-Field Splitting, $\left\{ \bar{S}_k \, \hat{\bar{D}}_{km} \, \bar{S}_k \right\}$
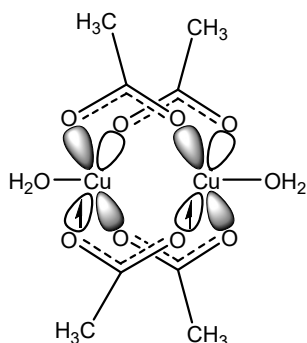
In the case of copper acetate, a basic spin system description combines an anisotropic g-tensor, a large hyperfine interaction of the [63,65]Cu nuclei, zero-field interactions, and exchange. Zero-field splitting will be considered first. In copper acetate this involves primarily the singly-occupied d_{x2-y2} orbitals of the two ions. The energy of two spin dipoles is conventionally written as

$$\Delta E = \frac{\mu_0}{4\pi}\left[\frac{\boldsymbol{\mu}_1 \cdot \boldsymbol{\mu}_2}{r^3} - 3\frac{(\boldsymbol{\mu}_1 \cdot \mathbf{r})(\boldsymbol{\mu}_1 \cdot \mathbf{r})}{r^5} \right]$$, and substituting $\boldsymbol{\mu} = \boldsymbol{g}\mu_B \hat{S}$, this is

converted to the zero-field splitting Hamiltonian (also dipole hyperfine, $\hat{I} \cdot \hat{S}$):

$$\hat{H}_{ZFS} = \frac{\mu}{4\pi}\boldsymbol{g}^2 \mu_B^2 \left[\frac{\hat{S}_1 \cdot \hat{S}_2}{r^3} - 3\frac{(\hat{S}_1 \cdot \mathbf{r})(\hat{S}_2 \cdot \mathbf{r})}{r^5} \right]$$, or in a more compact version

$\hat{H}_{ZFS} = \hat{S}\hat{\bar{D}}\hat{S}$. In the pre-lab exercise 4b, a triplet spectrum is given with points demarcated X, X', Y, Y', Z, and Z', where the primed and unprimed letters represent two overlapping powder patterns correspond to the $m_s=-1\rightarrow m_s=0$ and $m_s=0 \rightarrow m_s=1$ transitions. These correspond to the unique directions of the zero-field

splitting tensor, $\hat{\bar{D}} = \begin{pmatrix} -X & 0 & 0 \\ 0 & -Y & 0 \\ 0 & 0 & -Z \end{pmatrix}$. Using a definition of the zero-field splitting in terms of axial and

rhombic components, X, Y, and Z can be redefined as $-X = \frac{1}{3}D - E$, $-Y = \frac{1}{3}D + E$, and $-Z = -\frac{2}{3}D$. Thus

the energy splitting of Z and Z' is 2D and if E = 0, the energy splitting of X,Y and X',Y' is D, i.e. ZFS is axial. If E ≠ 0, the splittings of X to X' and Y to Y' are D ± E/3 and ZFS is orthorhombic. By adding an isotropic Zeeman interaction, with anisotropy defined by the ZFS tensor, the zero-field splitting term is expanded in the *zero-field basis* $|S,M_S\rangle$: {$(|1,+1\rangle-|1,-1\rangle)/\sqrt{2}, (|1,+1\rangle+|1,-1\rangle)/\sqrt{2}, |1,0\rangle$ } shown below, i.e. these states are linear combinations of the *high-field basis*, {$|1,+1\rangle, |1,-1\rangle, |1,0\rangle$}

$$\hat{H}_{ZFS} = \begin{pmatrix} \frac{1}{3}D - E & g\mu_B B_0 n_z & -ig\mu_B B_0 n_y \\ g\mu_B B_0 n_z & \frac{1}{3}D + E & g\mu_B B_0 n_x \\ ig\mu_B B_0 n_y & g\mu_B B_0 n_x & -\frac{2}{3}D \end{pmatrix}$$

Zero-field Hamiltonian including Zeeman interaction, in the zero-field basis.

CW-ESR Signal amplitudes

ESR of thermally isolated spin manifolds are proportional to the bulk magnetization of the paramagnetic centers in the sample, following the Curie Law.

$$\chi_0 = N_0 \frac{\gamma^2 h^2 B_0 S(S+1)}{3k_B T} \tag{1}$$

Here, χ_0 is the magnetic susceptibility, N_0 is the number of spins, γ is the magnetogyric ratio, B_0 is the external magnetic field, S is the spin number and k_B is the Boltzmann constant and T is temperature. In this sense, ESR is a quantitative technique. However quantitation in ESR often has an error of at least 3-10% due to instrumentation and sample preparation concerns. Integration of the ESR spectrum twice will provide a bulk magnetization value. An essential feature of Eqn. 1 is that the signal is inversely proportional to temperature and exactly proportional to the number of spins, N_0. In the absence of complicating factors such as thermal population of low-lying excited states, it is straight-forward to quantify the number of spins of a given species with a standard that fills the resonator active volume in the same way. For example, one common standard is a sample of 1 mM ethylenediaminetetraacetato-copper(II), a.k.a. CuEDTA, at pH = 4.0 in solution with about 30% glycerol. The signal amplitudes are also proportional to the Boltzmann populations of the spin levels. For an S=1/2 spin, or doublet, there are only two spin levels. However, in higher-spin molecules, e.g. Mn(II) is most often S = 5/2 with $m_S = \pm 1/2$, $m_S = \pm 3/2$ and $m_S = \pm 5/2$ spin manifolds, temperature can dramatically affect the spectrum by altering the relative intensities of transitions between spin manifolds.

Lorentzian Lineshape, 9.5GHz; T_1=500μs; T_2=1.5μs

While the overall ESR signal is proportional to the static magnetic susceptibility, χ_0, an ESR signal is described in terms of the dynamic susceptibility, $\chi = \chi' - i\chi''$, of the ESR sample. The dynamic susceptibility of isolated electron spins has two components that are dispersion and absorption, respectively:

$$\chi' = \frac{\gamma B_1 \chi_0 (\omega_0 - \omega) T_2^2}{1 + T_2^2 (\omega_0 - \omega)^2 + \gamma^2 B_1^2 T_1 T_2} \qquad (2a) \qquad \chi'' = \frac{\gamma B_1 \chi_0 T_2}{1 + T_2^2 (\omega_0 - \omega)^2 + \gamma^2 B_1^2 T_1 T_2} \qquad (2b)$$

The ordinate of a standard field-modulated ESR spectrum is dχ''/dB, i.e. it reports the derivative of absorption due the fact CW-ESR employs phase-sensitive detection by means of modulating the DC magnetic field (Pre-lab Q3). In equations 2a and 2b, ω_0 is the central resonant frequency and ω is a frequency +/- ω_0, where $\omega = 2\pi*v(MHz)$ is angular frequency in units of radians per second. B_1 is the applied microwave field strength (orthogonal to the main magnetic field, B_0) and T_1 and T_2 are the spin-lattice and spin-spin relaxation times. For ESR spin systems it is most-often the case that spin-spin relaxation (T_2 is generalized in practice to T_m, the phase memory time) is too fast for FID detection like NMR, especially at room temperature, hence CW-ESR has remained an essential ESR measurement technique for more than 70 years! If the microwave field strength is too great with respect to the relaxation rate, the ESR signal will be saturated because a significant number of spins have not completely returned to thermal equilibrium prior to measurement. It follows from Eqns. 2, that a saturation factor, s, can be determined from the relaxation rates of T_1 and T_2 and the microwave field magnetic induction, B_1.

$$s = \frac{1}{1 + B_1^2 \gamma^2 T_1 T_2} \qquad (3)$$

Eqn. 2b may be combined with some instrumental concerns to yield the signal voltage.

$$V_s = \chi'' \eta Q \sqrt{P Z_0} \qquad (4)$$
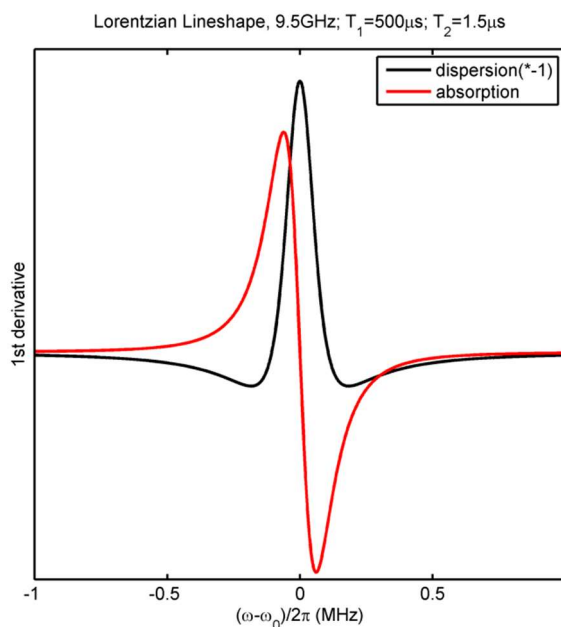
The signal voltage (V_s) is proportional to the absorption of microwaves by the sample, χ'', the filling factor of the resonator with sample (η), the resonator Q-factor and the square of microwave power (P) multiplied by the characteristic impedance of the transmission line (Z_0). The Q-factor is defined as 2π*energy stored/energy released per cycle, and it is a widely applicable property used in many diverse fields, such as laser cavities (e.g. Q-switching) and mechanical resonators (e.g. carbon nanotubes and tuning forks).

ESR intensities of thermally populated spin states, e.g. anti-ferromagnetic triplet states, often employ the Bleaney-Bowers equation in analysis, k is the Boltzmann constant, T is temperature modified by Weiss to include intermolecular interactions with θ, J is the exchange coupling for the singlet-triplet gap, and N_α is temperature independent paramagnetism. Note, the temperature of maximum susceptibility is about J/k.

$$\chi_0 = \frac{N_0 g^2 \mu_B^2}{3k(T-\theta)} \times \frac{1}{[1 + e^{-2J/kT}/3]} + N_\alpha$$

There are a few other instrumentation parameters that the effect signal voltage. One is the receiver gain, which multiplies the voltage prior to digitization. Commercial spectrometers provide field modulation rates between 10 to 100 kHz and the signal amplitude has a linear dependence on modulation amplitudes in the available range of 0.01 and 20 Gauss, regardless of frequency.

As B_1, the oscillating microwave field, is perpendicular to B_0, the DC magnetic field, the <u>signal amplitude</u> of a transition is proportional to the population difference times the square of the matrix element:

I_{ESR}(a.u.) $\propto (p_{Ms',MI'} - p_{Ms,MI})|\langle M_S',M_I'|\hat{S}_x|M_S,M_I\rangle|^2$ with the ESR <u>selection rules</u> of ΔM_S=1 and ΔM_I=0.
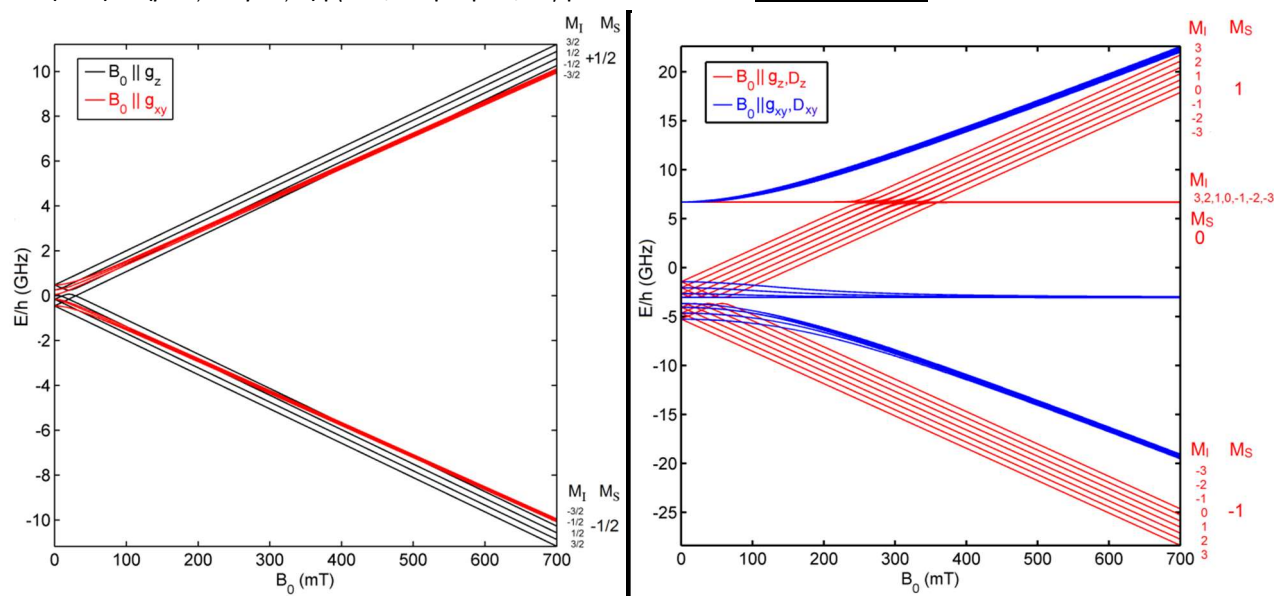
Figure 1. Representative energy level diagrams (spin Hamiltonian *eigenvalues*) for the Zeeman field effect on a single tetragonal ^{63}Cu, left S = 1/2, and exchange coupled di-^{63}Cu, right S = 1, for the sweep range of a basic X-band electromagnet. The high-field representation of M_I, M_S values is provided to the right of each.

Exercise: At X-band, the resonator frequency is often 9.4 GHz, so $\Delta E/h$ = 9.4 GHz. What is the length of that frequency difference on the y-axis of the lefthand plot? _____ mm. If you draw the vertical length from the upper red lines to the lower red lines, what field does the transition occur? _____ mT.

_____ Materials _____

> >/= 10L of liquid nitrogen in 60L dewar

> Small dewar of liquid nitrogen for freezing samples

> Two ESR samples flame-sealed in Wilmad 707-SQ-250M, (3mm I.D. x 4 mm O.D.) quartz tubes:
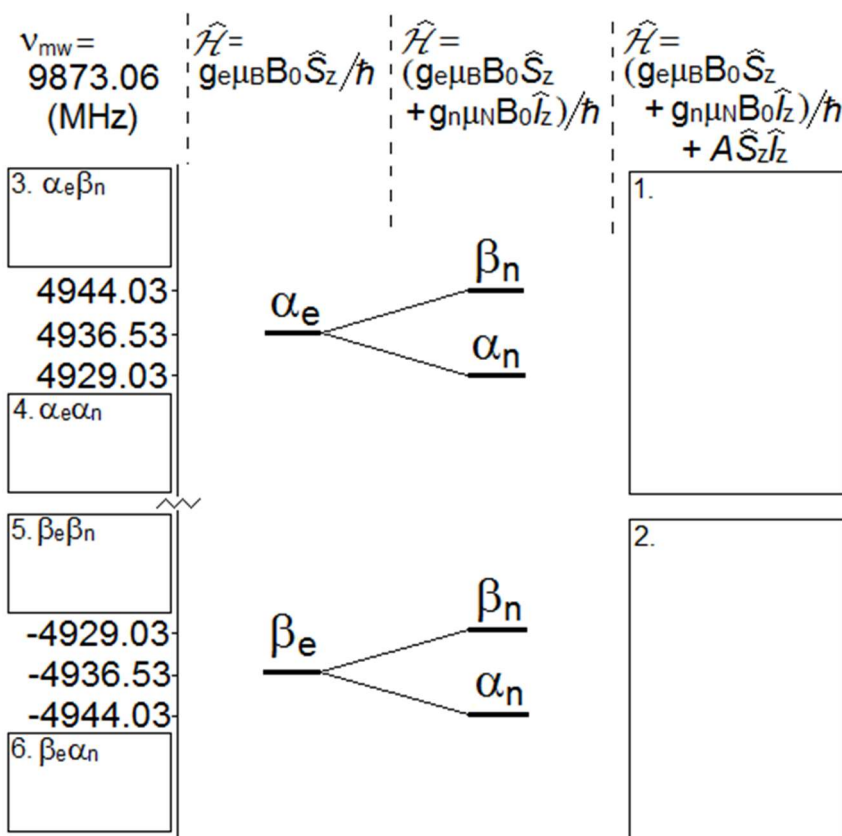
>> a. 200 uL of 8 mM CuTPP in toluene

>> b. powder of copper acetate

Pre-lab Assessment

Prior to answering the Prelab questions read through the practical sections and review magnetic resonance course notes to clarify the sequence of work and appropriate theory.


Q1. Why is ESR still mostly measured by continuous-wave spectrometers, the instrument design that NMR stopped using ca. 50 years ago?

Q2. The following diagram is for an isotropic $S=1/2$, $I=1/2$ spin system with the electron Larmor frequency ($\omega_{mw}/2\pi$) as indicated. In this case, the hyperfine splitting can be written AS_zI_z. For $A=3.4$ MHz, draw the levels for the $\alpha_e\beta_n$, $\alpha_e\alpha_n$, $\beta_e\beta_n$, and $\beta_e\alpha_n$ states in boxes 1 & 2 and enter the calculated energies in boxes 3, 4, 5, & 6. This nomenclature is that $m_S=1/2$ is α_e, $m_S=-1/2$ is β_e, $m_I=1/2$ is α_n, $m_I=-1/2$ is β_n. Indicate the difference in frequency for the two allowed ESR transitions: _____ MHz.

$\nu_{mw}=$ 9873.06 (MHz)

$\hat{\mathcal{H}}= g_e\mu_B B_0 \hat{S}_z/\hbar$

$\hat{\mathcal{H}}= (g_e\mu_B B_0 \hat{S}_z + g_n\mu_N B_0 \hat{I}_z)/\hbar$

$\hat{\mathcal{H}}= (g_e\mu_B B_0 \hat{S}_z + g_n\mu_N B_0 \hat{I}_z)/\hbar + A\hat{S}_z\hat{I}_z$

3. $\alpha_e\beta_n$

4944.03
4936.53
4929.03

4. $\alpha_e\alpha_n$

α_e → β_n, α_n

1.

5. $\beta_e\beta_n$

-4929.03
-4936.53
-4944.03

6. $\beta_e\alpha_n$

β_e → β_n, α_n

2.

Q3. For a sample containing unpaired electrons, what are situations where you might measure both the ESR and magnetic susceptibility using a SQUID magnetometer?

Q4. CW-ESR spectra most-often appear as a derivative. The external field amplitude is modulated over a small range by a set of coils, typically at 100 kHz. This allows separation of the ESR signal from microwave source noise $\left(\propto\left[frequency\right]^{-1}\right)$. The modulation reference frequency (Ref) is mixed with signal (Sig), where the relative phase θ gives this method its name, phase-sensitive detection = $0.5 * Amp_{Sig} \cdot Amp_{Ref}\left[\cos\left(\left(\omega_{Sig} - \omega_{Ref}\right)t + \theta\right) + \cos\left(\left(\omega_{Sig} + \omega_{Ref}\right)t + \theta\right)\right]$. The sum frequency is filtered-out. Below, the modulated signal amplitudes are at point a., $Sig(a) = a * \sin\left(\omega_{mod}t\right)$, at point b., $Sig(b) = b * \sin\left(2\omega_{mod}t\right)$, and at point c., $Sig(c) = c * \sin\left(\omega_{mod}t + \pi\right)$. The sine wave signal is *rectified*, given a low-pass filter and digitized, leading to the signal voltage.
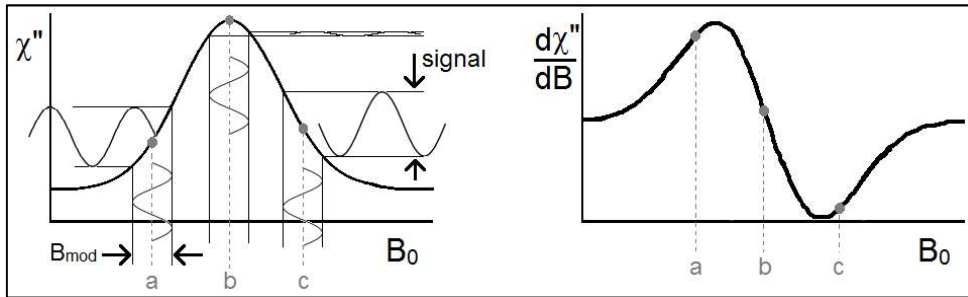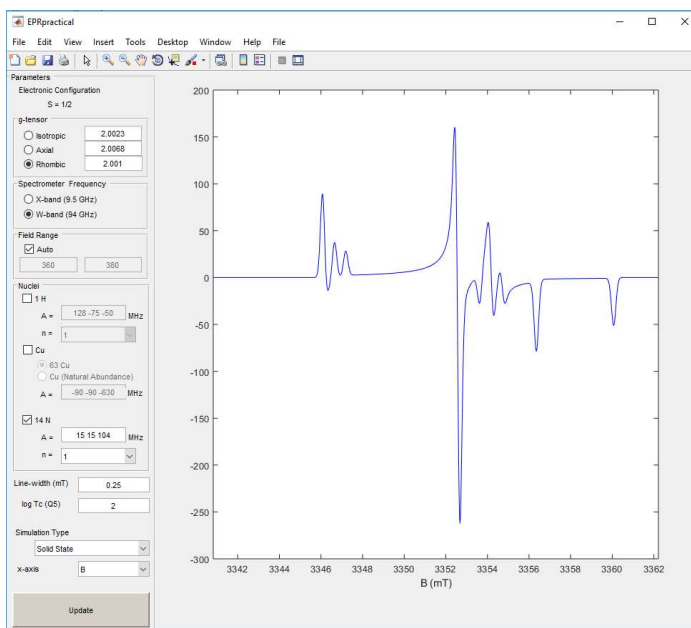

Given the absorption spectra on the left, draw the detected signals on the right:
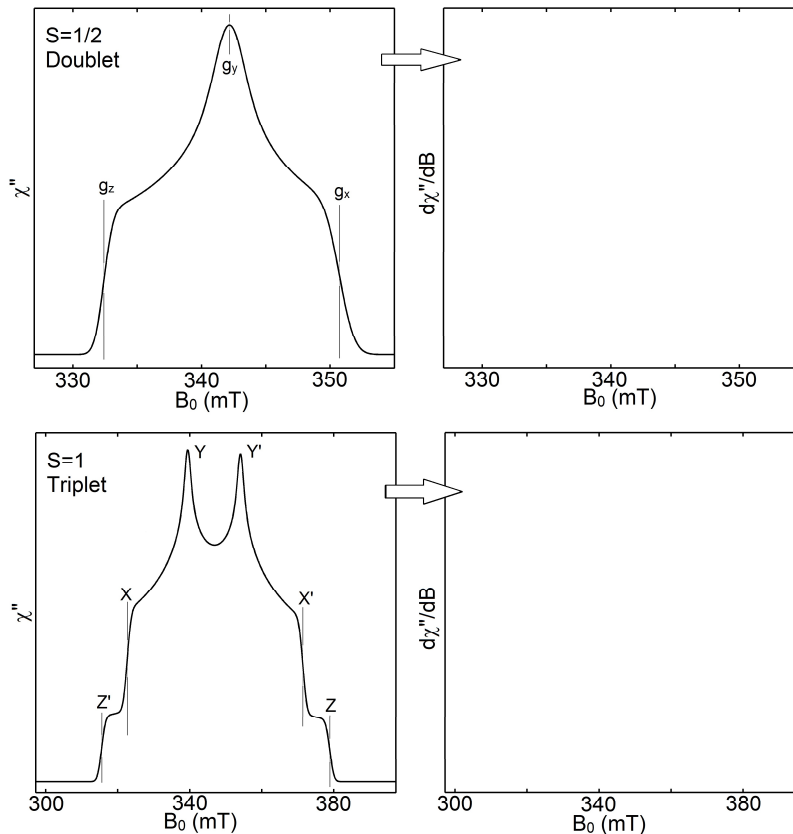
DAY 1 – COMPUTER-BASED EXERCISES

Simulation Exercises, part I

Using a computer provided to run an EasySpin toolbox installed in MatLab, or your own laptop, perform the following simulations to build towards understanding the spectral features of the samples measured in the ESR practical. EasySpin is a package of routines that is freely available from http://www.easyspin.org. Use of this software will allow you to develop a qualitative understanding of ESR simulations and provide guidance for theoretical aspects of ESR. These exercises utilize the EasySpin functions `pepper` for solid state ESR simulations and the function `chili` for slow motional ESR. See Appendix C for plotting code. For questions 1-to-5, you may use the GUI provided (EPRpractical.m) and/or any pre-written scripts in the ESR practical student directory; however, the ability to write your own scripts is an essential skill in ESR spectroscopy. You can save plots and collect them in a MS Word document for post-lab discussion.

1. Perform representative X-band simulations (9.5 GHz) with g-tensors that are characterized as

   a. isotropic   -- 1 resolved g-value

   b. axial   -- 2 resolved g-values

   c. orthorhombic   -- 3 resolved g-values

```
% isotropic simulation
clear all; clc;           % workspace, commands
sys.S = 1/2;                  % spin quantum number
sys.g = [2.0023 2.0023 2.0023]; % isotropic g-tensor, starting point
sys.lw = 0.5;                      % linewidth in mT
exp.mwFreq = 9.5;                  % microwave source frequency in GHz
exp.Range = [325 350];       % field sweep range in mT
opt.Method = 'perturb';
[x,y] = pepper(sys,exp,opt);  % run calculation with output variables
figure(1); clf; plot(x,y)      % basic plot
```
See plotting code on last page of Appendix C for more plotting tips. Save your spectra.

2. With g = [1.999 2.0023 2.0068] and a Gaussian linewidth of 2 mT, what is the minimum microwave source frequency to resolve the g-tensor? Why would you want to plot on a g-value axis instead of a field axis? *You might use this* `for` *loop:*   the following is useful $h/\mu_B \cong 71.447735$ mT/GHz

```
freqs=10:10:100;               % array of frequencies (start:step:end)
nf=numel(freqs);               % number of values in array
for ii=1:nf
    exp.mwFreq=freqs(ii);
    L=71.447729*exp.mwFreq/max(sys.g)-5*(sys.lw);
    R=71.447729*exp.mwFreq/min(sys.g)+5*(sys.lw);
    exp.Range=[L R];                          % Range is scaled to frequency
    [x,y]=pepper(sys,exp,opt);                % perform calculations
    Y(:,ii)=y'/max(y)+ii*0.25;        % y-data is saved as a 2D array
    X(:,ii)=71.447729*exp.mwFreq./x;   % x-data is saved as a 2D array
    text(1.985,ii*0.25+0.09,num2str(freqs(ii))); hold on; % label each trace
end
    % additionally, after plotting X,Y:
set(gca,'xdir','reverse');   % reverses x-axis direction as g-values are ∝ 1/B₀
```

3. For the axial case of g = [2.05 2.05 2.2], perform a simulations with a linewidth of 0.1 mT for a) the g-tensor alone, b) with a 100% ^{63}Cu hyperfine $A(^{63}Cu)$ = [-90 -90 -630]/MHz; c) with a natural abundance of Cu. d) For the 100% ^{63}Cu case, use simulations of single crystal orientations to assign peaks at X-band (9.5 GHz) and W-band (94 GHz) as shown below. Note that if you make your own total simulation, multiply by each angle by sinθ for the powder pattern. Try including, for example exp.nPoints ≥ 2^{12}.

```
angle = 0:0.05:90;
for ii = 1:length(angle);
    exp.CrystalOrientation=[0 angle(ii) 0]/180*pi;
    %% <- Your code here
    [x,y]=pepper(sys,exp,opt);          % perform calculations
    Y(:,ii)=y'/max(y)+ii*4;      % y-data is saved as a 2D stack
    Yno(:,ii) = y';              % y-data no stack offset
    Ysin(:,ii)=y'.*sin(exp.CrystalOrientation(2)); % y-data * sin(theta)
end
figure(3); subplot(2,1,1); pcolor(x',angle,Yno'); shading flat; colormap jet;
subplot(2,1,2); plot(x,sum(Ysin')); title('X-band A(63Cu)'); xlim(exp.Range);
```

Assign features in the ESR spectrum to m_I = 3/2, 1/2, -1/2, and -3/2 transitions, noting ΔM_S=1 and ΔM_I=0. How would you change the $A(^{63}Cu)$ values for the X-band spectrum to appear like the W-band spectrum?

4. The parameter values stated in exercise 3 are close that of CuTPP. By adding the ^{14}N hyperfine for CuTPP of $A(^{14}N)$ = [54 45 45]/MHz, _show_ and _explain_ the expected complexity of CuTPP of natural abundance Cu over just the lowest field M_I peak of Cu at $g_{||}$ by setting the field sweep range values from 273 to 286 mT. The splitting of the hyperfine features for identical hyperfine values should follow the rule of $2nI+1$, where n is the number of nuclei, and I is the nuclear spin. Note the influence $g_n(^{63}Cu)$=1.4849 and $g_n(^{65}Cu)$=1.5877, according to an isotropic hyperfine interaction. Start with ^{63}Cu, then switch to natural abundance Cu, and in a series of simulations, sequentially add 1-to-4 ^{14}N.

   Set field range from 265 to 288 mT. Start with 0.25 mT linewidth and in the final try also 0.75 mT.

5. The first part of these exercises deal with rigid-limit spectra where the molecule is frozen, i.e. tumbles at rates <u>very</u> much slower than the microwave frequency. When molecules spin at rates comparable to the microwave frequency, the sample is in the slow-motional regime. Alternatively, the molecule might tumble at rates much faster than the microwave frequency and this is described as the fast-motion limit, such as in room temperature NMR and small-molecule ESR in low-viscosity solvents. An estimate for the rotational correlation time (average motion to 1 radian) comes from the Stokes-Einstein equation.

$$\tau_r = \frac{1}{6D_{rot}} = \frac{4\pi\eta R^3}{3k_BT} \tag{5}$$

Here, η is the solvent viscosity (toluene 0.59 centiPoise) and R is the hydrodynamic radius of the molecule (about 7.3 Å for CuTPP). What is your estimate of τ_r for CuTPP? _____ What is $\log_{10}$ of that value (=_logtcorr_) _____ ? Using the function `chili` and the parameter values from exercise #3 (without nitrogen hyperfine),

   a) First make a plot of the spectrum with your calculated correlation time based on the microwave frequency (ν_{MW}) of 9.4 GHz. What is the _logtcorr_ value _____ ?

   b) Make a stack plot, of _logtcorr_ varied from -11 to -7 (enter -11:-7 in GUI), how do the spectra change?

This problem requires systematic variation of `sys.logtcorr` _(see Appendix C, pg. 31). You may need to increase opt.knots = 90; and_ `opt.LLKM  = [32 20 10 10];` _for elimination of artifacts. Simulations may take several minutes, especially with_ ^{63}Cu _hyperfine._

Simulation Exercises, part II

6. Following the Prelab Q2, simulations may be performed directly in the absence of a simulation package. The spin Hamiltonian, H = H_{EZ} + H_{NZ} + H_{HF}, is where the three terms are the electron Zeeman, nuclear

Zeeman, and hyperfine interactions.
$$\hat{H} = g_e \mu_B B_0 \hat{S}_z + g_n \mu_N B_0 \hat{I}_z + A\hat{S}_z \hat{I}_z + \frac{A}{2}(\hat{I}_- \hat{S}_+ - \hat{I}_+ \hat{S}_-)$$

a. Calculate energy levels of S = 1/2, I = 1/2 for A = 1420 MHz, B_0 range of 0 to 400mT, g_{eff} = 2.00294, g_n = 5.58569. Label energy levels in the high-field limit and draw lines for the 9.4 GHz transitions.

H_{EZ} $+H_{NZ} + H_{HF}$	$\|\alpha\alpha\rangle$	$\|\alpha\beta\rangle$	$\|\beta\alpha\rangle$	$\|\beta\beta\rangle$
$\langle\alpha\alpha\|$	$+\frac{1}{2}g_e\mu_B B_0$ $-\frac{1}{2}g_N\mu_N B_0 + \frac{hA}{4}$	0	0	0
$\langle\alpha\beta\|$	0	$+\frac{1}{2}g_e\mu_B B_0$ $+\frac{1}{2}g_N\mu_N B_0 - \frac{hA}{4}$	$+\frac{hA}{2}$	0
$\langle\beta\alpha\|$	0	$+\frac{hA}{2}$	$-\frac{1}{2}g_e\mu_B B_0$ $-\frac{1}{2}g_N\mu_N B_0 - \frac{hA}{4}$	0
$\langle\beta\beta\|$	0	0	0	$-\frac{1}{2}g_e\mu_B B_0$ $+\frac{1}{2}g_N\mu_N B_0 + \frac{hA}{4}$

```
clear all; clc;

% Constants
geff=2.00294;          % H atom electron, isotropic
gn=5.585695;        % H atom nucleus
h=6.6261e-034;          % J.s  Planck's constant
muB=9.27400968e-24;  % J/T  Bohr magneton
muN=5.05078324e-27;  % J/T  nuclear magneton

% Variables
B0=(0:0.05:400)./1000;  % Magnetic flux density, T
A=1420.40575e6;          % isotropic hyperfine coupling, Hz
vmw=9400e6;              % microwave frequency, Hz

% get eigenvalues
for ii=1:numel(B0)
    H=[+0.5*geff*muB*B0(ii)-0.5*gn*muN*B0(ii)+h*A/4 0 0 0;...
        0 +0.5*geff*muB*B0(ii)+0.5*gn*muN*B0(ii)-h*A/4  h*A/2 0;...
        0 h*A/2 -0.5*geff*muB*B0(ii)-0.5*gn*muN*B0(ii)-h*A/4 0;...
        0 0 0 -0.5*geff*muB*B0(ii)+0.5*gn*muN*B0(ii)+h*A/4];
    [v,d]=eig(H);            % calculate eigenvalues (d) and eigenvectors(v)
    E(ii,:)=diag(d)./h;     % collect eigenvalues for each field value
    d41(ii,:)=E(ii,4)-E(ii,1);   % differences
    d32(ii,:)=E(ii,3)-E(ii,2);
end

figure(1); clf;
plot(B0*1e3,E./1e9);        % mT vs. GHz
xlabel('B_0 (mT)');
ylabel('E/h (GHz)');
```

6. b. Make an X-band ESR spectrum (9.4 GHz) with a Lorentzian linewidth of 0.5 mT, using convolution. Append this code to your 6. A. script and adjust as required. After determining the resonance field for the two transitions, what is the difference in their polarization, P, where $P =$ tanh(geff$*\mu_B*B_0/kT$)? How you might use P in I_{ESR}(a.u.) $\propto$ ($p_{Ms',MI'} - p_{Ms,MI})|\langle M_S',M_I'|\hat{S}_x|M_S,M_I\rangle|^2$?

```
%% part b
y41 = interp1(d41,B0,vmw);   % interpolate to get resonance field
y32 = interp1(d32,B0,vmw);
Npts = 512*6;                              % number of x points
dB = (y32-y41)/(2/3*Npts-1); disp(dB*1e4);  % field step
Bnew = y41-Npts/6*dB:dB:y32+Npts/6*dB;     % new field axis
spc = zeros([numel(Bnew) 1]);
spc(Npts/6+1) = 1; spc(5/6*Npts) = 1; spc(Npts+1) = 0;  % make stick spectrum
FWHM = 6;                                   % Full-Width Half-Max
gam = FWHM/2/dB*1e-4;                        % gamma, correction factor
Ylz = gam^2./(gam^2+(-1*Npts/2:Npts/2).^2); % Lorentzian broadening function
spcL = ifft((fft(Ylz')).*(fft(spc)));      % perform convolution
spcL = fftshift(spcL);
spcL = spcL(1:Npts);
figure(2); clf;
plot(Bnew*1000,spcL,'k');
xlabel('B_0 (mT)');
ylabel('ESR Signal');
```

6. c. Consider now the *eigenvectors* as a function of field. What are they in very first few field points and how does this change as one approaches the field range for X-band ESR? Which field region best describes a coupled angular momentum *F*, where *F = I + S* ?

Try adding the following after `[v,d]=eig(M);` in the for loop of question 6. a. You might wish to reduce the number of B0 field points after first doing a trial of `for ii=1:1` *Note that re-ordering of columns may need further re-ordering for $B_0 = 0$ and other fields.*

```
  imagesc([v(4,4) v(1,1) v(1,3) v(4,2);...
           v(3,4) v(2,1) v(2,3) v(3,2);...
           v(2,4) v(3,1) v(3,3) v(2,2);...
           v(1,4) v(4,1) v(4,3) v(1,2)]); drawnow;
  text(1,4,num2str(v(1,4))); text(1.6,2,num2str(v(4,2)));
  text(2.6,2,num2str(v(2,1))); text(1.6,3,num2str(v(2,3)));
  text(2.6,3,num2str(v(3,1))); text(4,4,num2str(v(3,3)));
  pause(0.5);
```

6. d. You have calculated the *eigenvalues* and *eigenvectors* with variation of B0. It is possible for some spin systems to derive an analytical *eigenfunction* equation that describes the *eigenstate*. Try plotting the following on the figure of 6a., using `hold on;`

```
eig2 = 3/32*(-8*A*h/3+sqrt((256/9)*A^2*h^2+(256/9)*B0.^2*geff^2*muB^2+...
    (512/9)*B0.^2*geff*gn*muB*muN+(256/9)*B0.^2*gn^2*muN^2));

eig25 = -h*A/4+0.5*sqrt((geff*muB+gn*muN)^2.*B0.^2+A^2*h^2);
```

DAY2 – EXPERIMENTAL DATA ACQUISITION
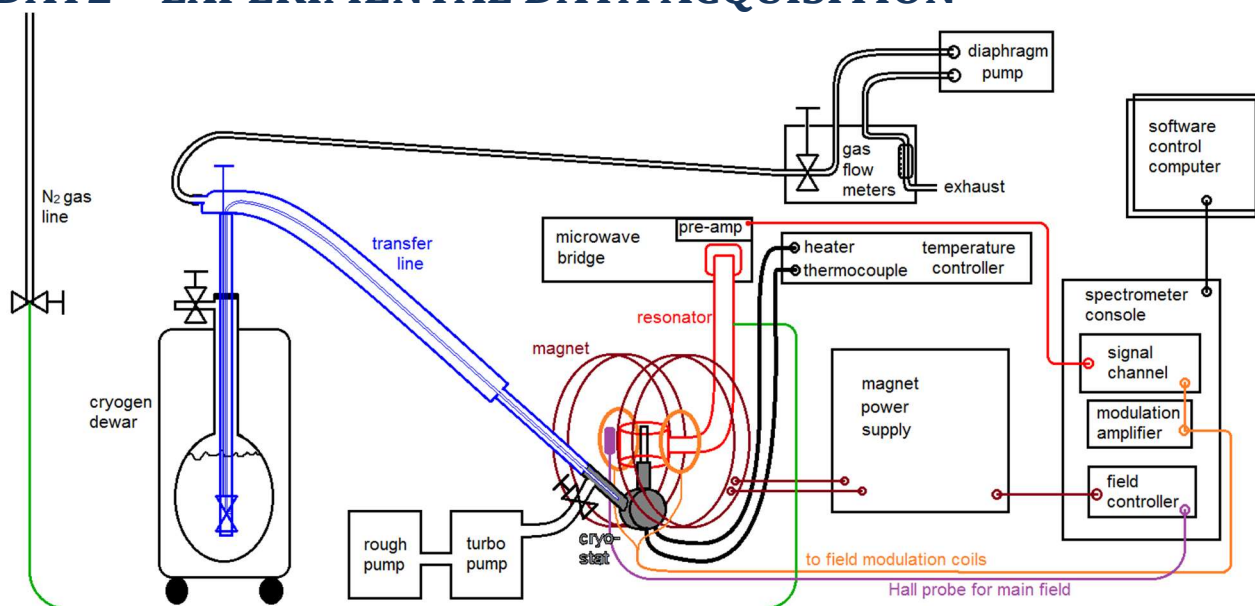
Spectrometer preparation

Work with the JD to identify spectrometer components, set up the cryostat with a $N_{2(l)}$ dewar for temperature of 100K, and warm-up the microwave bridge. First the ESR-900 cryostat should be set in the magnet. Switch the turbo pump on and it will engage the roughing pump, left on at all times, as required. Next, the cryostat valve is opened. This will remain opened for the duration of the experiment. You might need to fill the 60L N_2 tank (10-20L is enough). Insert the Oxford Instruments LLT-600 transfer line into the liquid N_2 tank with the assembly stack in place and closed.

Insert the transfer line into the EPR-900 cryostat and turn on the GAST G4 diaphragm pump with both the transfer line needle valve and the VC41 gas flow controller open several turns. Turn on the Oxford Instruments ITC-503S controller and set the temperature to 100K and the Proportional, Integral and Derivative (PID) to 15 K, 2.5 min., and 0.5 min. Then tighten-down the transfer line in the cryostat. Once gas flow of about 0.5-1 in L/Hr is achieved in the VC41, turn the transfer line needle valve down to about ½ turn open and start to turn down the flow at the VC41 to keep the vacuum as displayed by the VC41 in the range of 800-700 mBar (0 mBar on the VC41 scale is atmospheric pressure, ca. 1013mBar) to prevent formation of frozen N_2 blockages which occur in the VC41 displayed value of ca. 863 mBar. When the temperature passes below about 250K, switch from MANUAL on AUTO on the ITC-503S temperature controller. DON'T PRESSURISE TANK, the bleed valve "Wade" and adjacent bladder connection at the top of the liquid nitrogen dewar should be opened fully. The N_2 gas line is reduced to a light flow and attached it to the purge port on the back of the resonator waveguide. The heater should slowly increase to 20-30V as 100K is approached.

SAFETY: Safety glasses must be worn. Sudden release of cold N_2 gas from a pressurised liquid N_2 dewar or condensed atmosphere in a tube can cause severe cryogen burns, cryogenic gloves are essential for LLT-600 transfer line handling. Any pressure must be released with the bleed valve in a controlled manner by the JD <u>prior</u> to removal of the transfer line from the liquid N_2 dewar. *Students should not adjust the spectrometer hardware or change samples without the JD present*.

In this beginning part of the laboratory you will obtain ESR spectra of a ca. 2 mM CuTPP solution at 100 K. For insertion of the sample to a cryostat below its melting point (toluene, 178 K), the sample is first frozen in liquid N2. If the cryostat is above the freezing point, the sample should be inserted in liquid form. Insertion of a frozen sample into a warm, flowing cryostat will result in a broken tube due to primary melting and expansion of the organic solvent from the bottom first. Typically one would follow the sample containing an analyte with a solvent blank, but in this case, we've found that the background is of negligible intensity with respect to the ESR signal.

It is your first objective to obtain a high quality spectrum under non-saturating conditions. The CuTPP sample should be mounted in the sample stack connector and then frozen slowly in liquid nitrogen from bottom to top at vertical insertion rate of about 1 mm per 2 sec. Switch off the diaphragm floor pump, let the vacuum in the cryostat return to zero, insert your frozen sample, and turn the pump back on again. After allowing the temperature of the sample to equilibrate, complete spectrometer tuning with the instructions on the following page. The ESR signal is measured with a reflection resonator. The absorption of microwaves by the sample, i.e. sample resonance, fundamentally alters the free passage of microwaves into the resonator. This induced imbalance results in reflected microwave power toward the detector diode.

It is important to be familiar with the decibel scale for a 200 mW microwave source:

$$\underline{10\ dB}\ of\ Attenuation = -10dB = 10*\log_{10}(P_{out}/P_{in}) = 10*\log_{10}(\underline{20mW}/200mW)$$
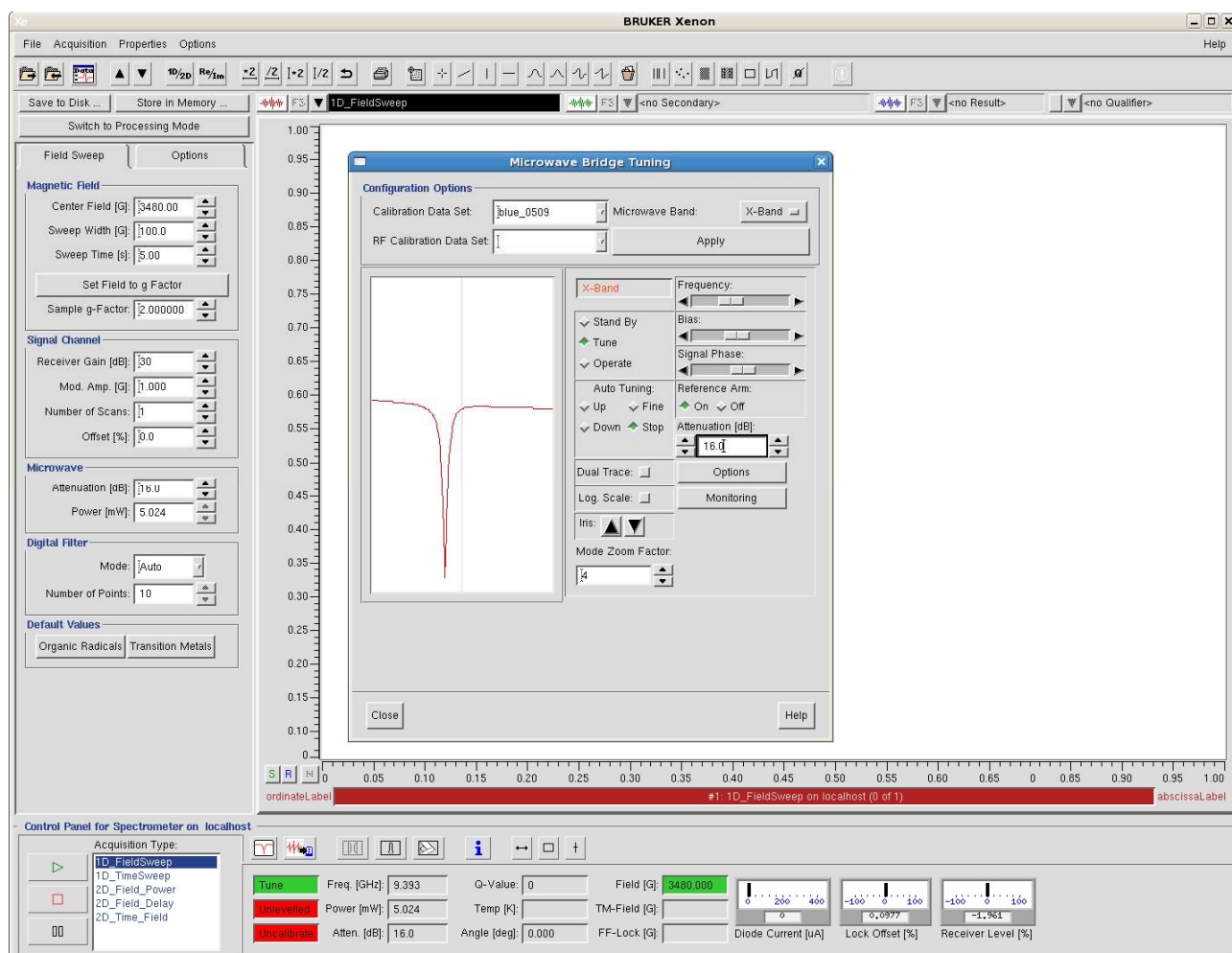
The ESR spectrometer software interface in Tune Mode, showing resonator "dip". Find dip icon.
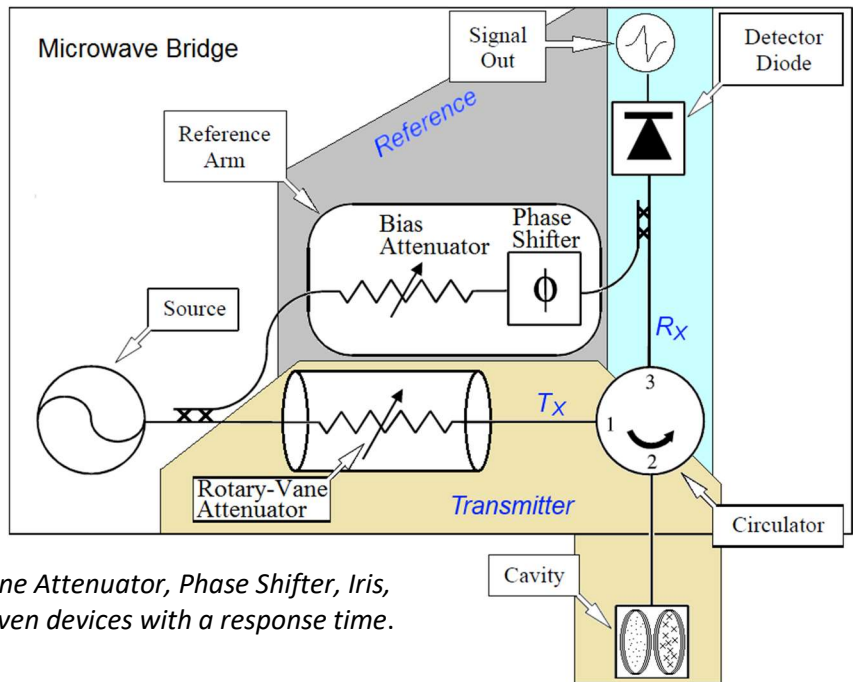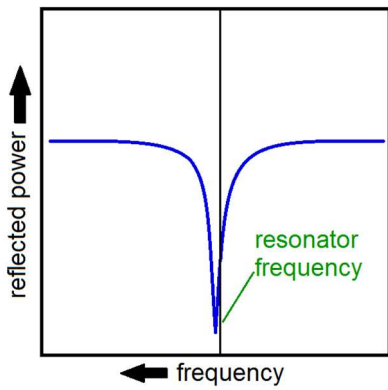
CW-ESR Tuning Procedure

Please note that that the Rotary Vane Attenuator, Phase Shifter, Iris, and Frequency are mechanically-driven devices with a response time.
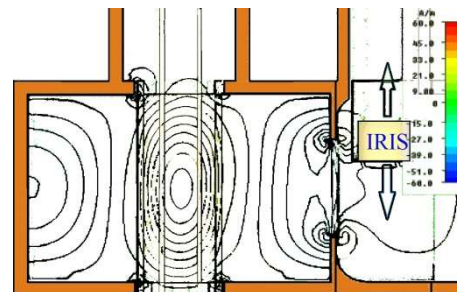
(1) Switch on Tune Mode

Look for dip icon in lower left part of screen

(2) Set B_0 field off-resonance

Perform tuning at a field position
without an ESR signal.

(3) Turn Reference Arm off

First, the reflections from the cavity are
minimized in isolation from reference.

(4) Set Attenuation to 20dB, find dip
using the Frequency slidebar.
Center dip on center line,
using the Mode Zoom Factor as required.

Cryostat + blue or black resonator
~ 9.4 GHz
Empty blue resonator ~ 9.8 GHz
Empty rectangular resonator ~ 9.7 GHz

(5) Use the Iris to minimize reflected power at
resonator frequency

(6) Turn Reference Arm on, with Bias in middle
(7) Set Attenuation to 30dB and
use Phase to get a symmetric dip
(8) Set Attenuation to 20dB and go to Operate Mode

(9) Center AFC *Offset* percentage within
~ +/-15% w/ Frequency slider

(10) Set Attenuation to 60dB

This shuts down Transmitter Arm,
-60dB= 1/1,000,000; -3dB=1/2; -6dB=1/4.

(11) Use Bias to get 200µA in *Diode Current*

200µA is the center of linear detection

(12) Set Attenuation to 20dB, center *Diode* with Iris
(13) Set Attenuation to 10dB, center *Diode* with Iris

(14) Use Signal Phase to maximize *Diode*

maximize phase coherence of reference and
transmitter paths at the diode

(15) Re-center *Diode* at 200µA w/ the Iris as necessary
(16) Check Tuning at Attenuations from 10dB to 50dB in steps of 10dB
Re-center diode with Iris as necessary
(17) Switch on Tune Mode
(18) Set attenuation at 33dB and wait for a
green Q-value measurement
(19) Set attenuation at 23dB and
switch on Operate Mode … *done*!
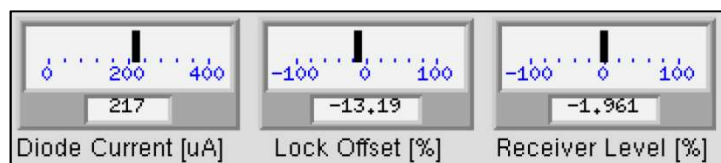
============= Acquisition Optimization =================

First complete the previously described Tuning. *For CuTPP at 100K.*, determine the extent of the ESR signal in the Zeeman field sweep under moderately high microwave power and modulation amplitude, e.g. ~10mW and 10G, respectively, over a field sweep range of 100 to 7000G, with a sweep time of 120 seconds and a time constant of 20.48 msec (under the Options tab). Other samples have some given parameter values to expedite the signal acquisition optimization.

a. CuTPP (100K); b. CuAcetate (100K); c. CuTPP(200K);

1. ESR Signal Width (G)	a. _____	b. _____	c. _____	High field edge minus low field edge
2. Center of Signal (G)	a. _____	b. 3250	c. __*a.*___	Field value in middle of the signal
3. Sweep Width (G)	a. _____	b. 6300	c. __*a.*___	~ Signal Width + 20*narrowest feature
4. Narrowest Feature (G)	a. _____	b. _____	c. _____	FWHM or peak-peak width
5. Mod. Ampl. (G)	a. _____	b. __4__	c. __*a.*___	0.3 of narrowest feature
6. Sweep Time (sec)	a. _____	b. _140_	c. __*a.*___	~10-50 Gauss/ sec., or 1-10 min.
7. Time Constant (ms)	a. _____	b. 40.96	c. __*a.*___	$1/10^{th}$ time to pass narrowest feature

→Perform a sweep under these conditions. You may need to iteratively change the narrowest feature and modulation amplitude and perform some intermediary sweeps.

   Then set the field to the maximum signal intensity point in the spectrum by clicking and dragging the green vertical field marker in the spectrum. Temporarily set the time constant to 655 ms. Go to 10 dB attenuation and set the receiver gain such that the receiver level is somewhere between +/- 60-80%. Find a point in the field sweep range where there is no ESR signal intensity and make sure that the signal level is at zero by using the offset.

Selected Microwave Power Optimizations (*receiver level %*)					
Microwave attenuation (dB)	10	16	22	28	34	40
Microwave power (mW)						
CuTPP (100K)						

|				
8. Microwave Atten. (dB)	a. _____	b. __22_	c. __20_	non-saturated at $\Delta Signal = (\Delta Power)^{0.5}$
9. Receiver Gain (dB)	a. _____	b. __41_	c. _____	Max |Signal| to +/- 60-80% of Receiver

===

Once you establish the sweep widths, proceed with optimizing modulation amplitude by finding your narrowest feature and reducing the modulation amplitude until the feature doesn't change in width. Under exacting conditions, an undistorted lineshape would require a modulation amplitude of about $1/10^{th}$ the line width, here we recommend $3/10^{ths}$ of the narrowest feature to reduce signal averaging time. A choice of microwave power is obtained by finding a power where the signal amplitude is linear with the square root of the microwave power. An expedient method of

microwave power optimization is to decrease the microwave power in 6dB steps from a low attenuation value until the ESR signal changes by a factor of two each time, and the above table may be used for that purpose. Alternatively, one may measure a two dimensional data set of field and power.

$$S = K\sqrt{P}/\left[1 + \left(P/P_{1/2}\right)\right]^{b/2} \tag{6}$$

In Eqn. 6, the relation of ESR signal amplitude (S), which can be defined as the signal amplitude at a single field value, is shown relative to the microwave power (P), using a scalar (K), the value of microwave power for half-saturation ($P_{1/2}$) power, and a homogeneity factor (b).
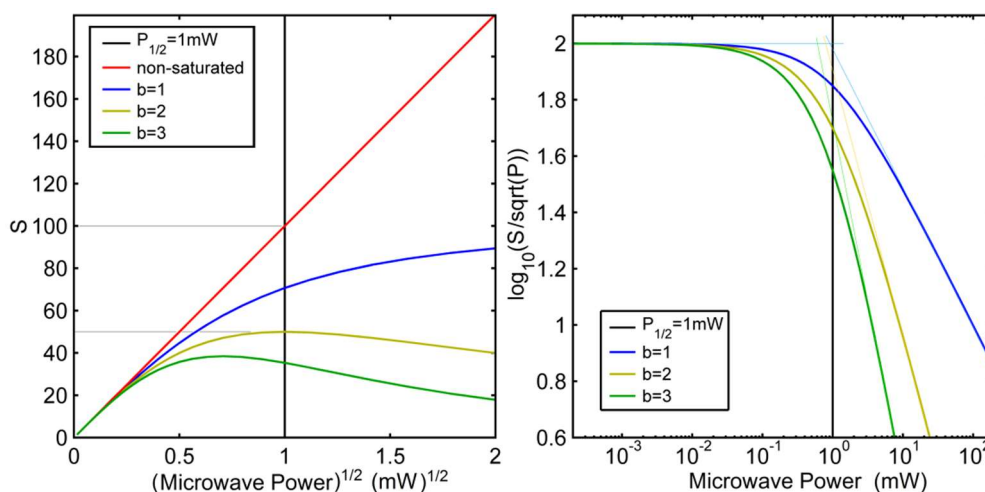
Figure 2. Plots of Eqn. 6, at limits of b = 1 for inhomogenous broadening of ESR lines, an intermediate case of b = 2 and at a limit of b = 3 in the case of homogeneous broadening. The plot on the right shows a graphical means of estimating the half-saturation power.

Acquisition summary:

	Temp(K)	Sample	Scans	Comments
1.)	100K	CuTPP	12	FREEZE the sample prior to insertion
2.)	100K	CuAcetate	1	Use provided parameter values
3.)	200K	CuAcetate	1	Same as #2
4.)	200K	CuTPP	4	DON'T freeze sample prior to insertion.
5.)	300K	CuTPP	4	Same as #4
6.)	300K	CuAcetate	1	Same as #2

Exit checklist:

Email yourself the following, in a compressed ZIP file:

ESR spectra for all acquisitions, converted to tab-delimited ascii files by JD.

UV-Vis data for Post-lab question 1.

Simulated spectra for Post-lab question 2.

Q1. Frozen solution measurement of CuTPP

(Q1a) If you were to substitute the Cu(II) with low-spin Co(II), how would expect that to effect the ^{14}N hyperfines hyperfine interaction? Consider the energy levels of and occupations of the d-electrons.

(Q1b) Considering $A_{iso} = \dfrac{2\mu_0}{3h} g_e \mu_B g_n \mu_N \rho |\Psi_0|^2$, $= \rho$(1811 MHz), the isotropic ^{14}N hyperfine on a simplified level, what fraction (ρ) of the unpaired electron spin density is in the s-orbitals of the nitrogen ligands, individually and in total? Use the hyperfine values from Day 1, exercise 3, $A(^{14}$N$)$ = [54 45 45]/MHz. What is the remainder of spin density that may be associated with the Cu ion?

(Q1c) Following the Introduction discussion of excited state mixing and the information provided below, to what extent are you able to <u>assign *d-d* transitions in the optical absorption spectrum</u> with the g-values of Day 1, simulation exercise 3, g = [2.05 2.05 2.2]?
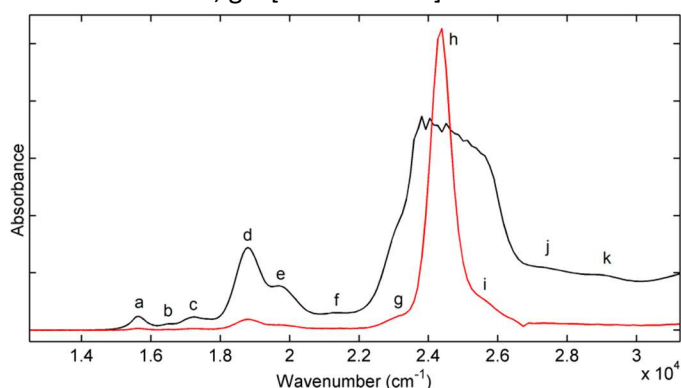

Figure 3. Optical absorption spectrum of CuTPP in toluene solution at two concentrations. Transitions in wavenumbers (cm^{-1}) are a.15625 b. 16647 c.17241 d.18797 e.19685 f.21367 g.23041 h.24390 i.25641 j.27322, and k.28901.

$$g_P = g_e - \frac{8\lambda\alpha^2\beta^2}{\Delta(b_{2g} - b_{1g})} \qquad (7a) \qquad\qquad g_\perp = g_e - \frac{2\lambda\alpha^2\delta^2}{\Delta(e_g - b_{1g})} \qquad (7b)$$

$$^{Cu}A_\parallel = P\left[-\kappa - 4/7\,\alpha^2 - 3/7\left(g_e - g_\perp\right) - \left(g_e - g_P\right)\right] \qquad (7c)$$

The free-ion spin-orbit coupling constant is $\zeta = -830\,\text{cm}^{-1}$, $\lambda = \pm\zeta/2S$, while α, β, and δ are covalency parameters, *vide infra*. **An initial guess** for the parameter values can come from the related molecule, phthalocyanatocopper(II). Phthalocyanine covalencies are the d_{x2-y2} orbital and ^{14}N σ-orbitals, $\alpha^2 \approx 0.76$, the d_{xy} orbital and porphyrin π-orbital, $\beta^2 = 1$, and the d_{xz} and d_{yz} orbitals and porphyrin π-orbital, $\delta^2 \approx 0.60$. The values are 1 for purely ionic bonding, but less than 1 for covalent bonding. The Fermi-contact term in equation 7c is $P\kappa$, where P is the dipolar coupling of the d-electron to the ^{63}Cu nucleus and κ is the orbital reduction factor. Note that $d-d$ transitions are weakly allowed via vibronic coupling in the distorted samples that lack a center of inversion. Assume that $\beta^2 = 1$ and $P = 1164$ MHz and use equations 7 to assign $\Delta(b_{2g} - b_{1g})$ and $\Delta(e_g - b_{1g})$ to peaks in the UV-Vis spectra data files provided and fine-tune values for α^2 and κ. You may select peaks based on the data files other than those indicated above.

(Q1d) There are twelve primary distortions of porphyrin rings, six out-of-plane, and six in-plane. In the case of a saddle distortion, two opposite pyrroles rings are lowered out-of-plane with respect to the alternate pyrrole-Cu(II)-pyrrole axis. Based on the orbital overlap equations of question (c), what is your qualitative prediction of the effect on ESR parameter values {g-values, $A_{\parallel}(^{63}$Cu$)$, $A(^{14}$N$)$} by increasing a saddle distortion?

saddle distortion
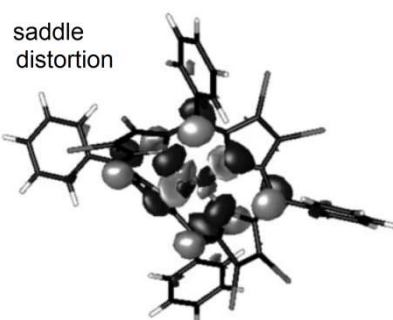
Q2. Slow-motion EPR of CuTPP

The JD will provide you with a series spectral simulations that use the experimental g-tensor and hyperfine tensor values as a basis for simulations that vary the rotational correlation time of the CuTPP at 200 K and 300 K. A help document for importing the data into MS Excel is included, *further notes are below and on next page*.

To have performed these simulations, first a slow-motion spectrum of only the g-tensor and Cu hyperfine interaction was calculated. Then a stick spectrum of the isotropic ^{14}N hyperfine was convolved with the Cu-only spectrum, similar to what you did in exercise 6b.

One of the simplest goodness-of-fit equations is a sum of the squares of errors:

$$Ssq = \sum_{i=1}^{N} \left(y_{Exp(i)} - y_{Sim(i)} \right)^2$$

Here, N is the number of spectrum points, $y_{Exp(i)}$, $y_{Sim(i)}$ are the ith intensity of the experimental and simulated spectrum, respectively ($i=1,\dots N$).

(**Q2a**) Make a plot of *Ssq* vs. τ_r for the 200 K data and the 300 K data. Identify the best correlation times for the CuTPP spectra measured at 200 K and 300 K. What are they in nanoseconds?

(**Q2b**) Make plots of the data, best fit and their difference for 200 K and 300 K (two plots, three traces each). Correctly label the axes, title and figure legend.

(**Q2c**) Given the following equation, explain trend the in rotational correlation times vs. temperature as determined in question Q2a.

$$\tau_r = \frac{4\pi\eta R^3}{3k_B T}$$

Further notes:

The documents you need for this are named as follows: taulist_200K.txt, taulist_300.txt, taur_200K.txt, taur_300K.txt as well as the data files for the two spectra at the different temperatures with a different extension, *.dat, which means *changing the display criteria* in the data import window. Two of the files contain simulations that vary the correlation time, they are tailored to the number of points for the 200 K and 300 K data you generated. The other two files are the tau values used in the simulations for 200 K and 300 K, given in $\log_{10}(\tau_r)$ as in simulation exercise.

You will need to import the 3 text files for each temperature into Excel (taulist, taur and the data file). A good way to set these out in Excel is the data file in A1, taur in H1 and taulist in D6.

To calculate SSQ use the 'B' column of the data file you imported (this is your yExp(i)) and compare it to each column H to X (this is your ySim(i)) using Eq. 8 of the simulation data.

Do this for the 200K case then repeat for the 300K case.

After import your spreadsheet should look something like this:

This is the simulation data from the file taur, in the SSQ calculation

each column represents a different y sim value

This is the data from the tau_list file.

This is the yexp value, with the data from the .dat file.

The calculation to get E7 was

=SUMXMY2(B:B,H:H)

|	A	B	C	D	E	F	G	H	I	J	K	L
1	244	-0.00089		200K				2.78E-06	5.39E-06	1.06E-05	2.02E-05	4.00E-
2	244.03	-0.00089						3.13E-06	6.08E-06	1.19E-05	2.28E-05	4.51E-
3	244.06	-0.00085						3.20E-06	6.20E-06	1.22E-05	2.32E-05	4.60E-
4	244.09	-0.00075						3.17E-06	6.14E-06	1.20E-05	2.30E-05	4.56E-
5	244.12	-0.00058						3.11E-06	6.03E-06	1.18E-05	2.26E-05	4.47E-
6	244.15	-0.00035		log_10(tau_r)	SSQ			3.04E-06	5.89E-06	1.16E-05	2.21E-05	4.37E-
7	244.18	-7.5E-05		-7.00581	117.4611			2.96E-06	5.74E-06	1.13E-05	2.15E-05	4.26E-
8	244.21	0.000194		-7.2560175				2.87E-06	5.57E-06	1.09E-05	2.09E-05	4.13E-
9	244.24	0.0004		-7.506225				2.78E-06	5.39E-06	1.06E-05	2.02E-05	4.00E-
10	244.27	0.000498		-7.7564325				2.67E-06	5.18E-06	1.02E-05	1.94E-05	3.85E-
11	244.3	0.000472		-8.00664				2.56E-06	4.97E-06	9.75E-06	1.86E-05	3.69E-
12	244.33	0.000346		-8.2568475				2.44E-06	4.74E-06	9.30E-06	1.78E-05	3.52E-
13	244.36	0.000186		-8.507055				2.32E-06	4.50E-06	8.83E-06	1.69E-05	3.34E-
14	244.39	7.56E-05		-8.7572625				2.19E-06	4.25E-06	8.34E-06	1.59E-05	3.15E-
15	244.42	8.68E-05		-9.00747				2.06E-06	3.99E-06	7.83E-06	1.50E-05	2.96E-
16	244.45	0.000238		-9.2576775				1.92E-06	3.73E-06	7.31E-06	1.40E-05	2.76E-
17	244.48	0.000485		-9.507885				1.78E-06	3.45E-06	6.77E-06	1.29E-05	2.56E-
18	244.51	0.000738		-9.7580925				1.64E-06	3.17E-06	6.22E-06	1.19E-05	2.35E-
19	244.54	0.000907		-10.0083				1.49E-06	2.89E-06	5.67E-06	1.08E-05	2.14E-
20	244.57	0.000933		-10.258508				1.34E-06	2.60E-06	5.11E-06	9.75E-06	1.93E-
21	244.6	0.000799		-10.508715				1.19E-06	2.32E-06	4.54E-06	8.67E-06	1.72E-
22	244.63	0.000524		-10.758923				1.04E-06	2.02E-06	3.97E-06	7.58E-06	1.50E-
23	244.66	0.000155		-11.00913	298.9017			8.94E-07	1.73E-06	3.40E-06	6.49E-06	1.29E-
24	244.69	-0.00025						7.44E-07	1.44E-06	2.83E-06	5.40E-06	1.07E-
25	244.72	-0.0006						5.95E-07	1.15E-06	2.26E-06	4.32E-06	8.55E-
26	244.75	-0.00082						4.47E-07	8.67E-07	1.70E-06	3.24E-06	6.41E-
27	244.78	-0.00085						3.00E-07	5.82E-07	1.14E-06	2.17E-06	4.29E-
28	244.81	-0.00066						1.55E-07	3.00E-07	5.88E-07	1.12E-06	2.20E-
29	244.84	-0.0003						1.15E-08	2.21E-08	4.30E-08	7.95E-08	1.41E-
30	244.87	0.000165						-1.29E-07	-2.51E-07	-4.92E-07	-9.42E-07	-1.88E-
31	244.9	0.000607						-2.67E-07	-5.18E-07	-1.02E-06	-1.94E-06	-3.87E-
32	244.93	0.000954						-4.01E-07	-7.79E-07	-1.53E-06	-2.92E-06	-5.80E-

Q3. Solid state ESR of copper acetate

This bimetallic system contains two strongly-coupled spins, with the zero-field splitting described by a dipolar component, $D_{dip} = -\left[2g_z^2 + \left(g_x^2 + g_y^2\right)/2\right]\mu_B^2/2r_{Cu\text{-}Cu}^3$, with r = 2.617Å. This question concerns estimation of *isotropic J*, representing the exchange coupling for the anti-ferromagnetic energy difference between the ground state singlet and excited triplet state manifold. For interest only, a more complete *anisotropic* exchange coupling that splits the zero-field energies of the singlet and triplet states is given as $D_{ex} = \left[J\left(x^2-y^2, xy\right)\Delta_z^2 - 2J\left(x^2-y^2, xz\right)\Delta_y^2 - 2J\left(x^2-y^2, yz\right)\Delta_x^2\right]/32$, where $\Delta_z = g_z - g_e$, $\Delta_y = g_y - g_e$, and $\Delta_x = g_x - g_e$, and $J(x^2\text{-}y^2, d\pi)$ is the exchange coupling between the d(x^2-y^2) orbital of one Cu(II) and the excited stated dπ orbital of the other Cu(II). ESR at many different frequencies up to 420 GHz was used to determine **g**=[2.0545 2.0792 2.3637] and **D** =[0.1014 0.1220 -0.2233]/cm^{-1}.
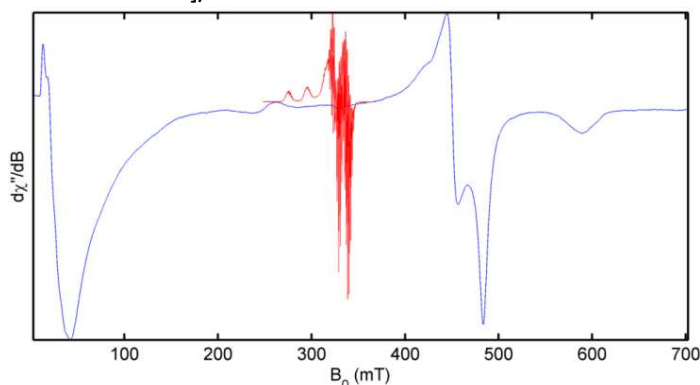
Figure 4. X-band ESR comparison of powders of 5% CuTPP in ZnTPP (red) and neat copper acetate (blue), collected at 125K and microwave powers of 0.2mW and 2.5mW, respectively. The microwave frequency is 9.3775 GHz.

(**Q3a**) Why is the red spectrum located only in the center of the spectrum, while the blue spectrum appears mostly on either side? Use Fig. 1 and the energy level diagrams below to label features in your 100 K copper acetate spectrum on the basis of D-tensor direction, x, y, & z. Draw vertical lines for transitions in the following and label the states according to $\hat{H}_{EZ} = \mu_B g_{eff} B_0 \hat{S}_Z$ and the high-field representation, |S,M$_S$⟩. Note that the zero-field representation involves taking linear combinations of eigenstates, e.g. (|S,M$_S$⟩±|S,M$_S$-1⟩)/√2. *Hint:* use a ruler for ν$_{mw}$ = 9.4 GHz between lines, it is $\Delta E = g\mu_B B_0$ and may have any offset on y-axis.
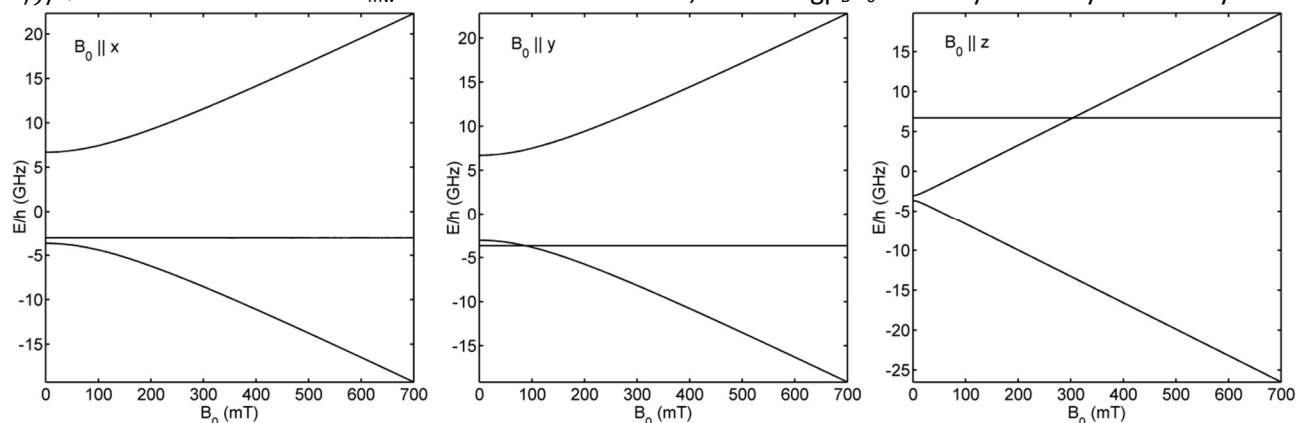
(**Q3b**) Subtract the minimum of the negative peak at ~590 mT from the baseline average of last 20 points ca. 700 mT for 100 K, 200 K, and 300 K and comment on the temperature dependence. Can you estimate a value for *J* by fitting the data with following equation? You may need to scale the data by an arbitrary constant, such as 3 x 10^{-4} (omits temperature-independent paramagnetism and monomers). Here: $\hat{H}_{ex}$ = $-J\hat{S}\cdot\hat{S}$

$$\chi_{\parallel} = \frac{0.735}{T}\left[1 + \frac{1}{3}exp(-J/k_B T)\right]^{-1}$$

References

1. Bagguley, D.M.S., Griffiths, J.H.E., Paramagnetic Resonance and Magnetic Energy Levels in Chrome Alum, *Nature* **1947**, *160*, 532-533.

2. Church, A.H., *Phil. Trans. Roy. Soc. London, Ser. A*, **1869**, *159*, 627-629.

3. CODATA, The Committee on Data for Science and Technology, http://www.codata.org

4. Cummerow, R.L., Halliday, D., Moore, G.E., Paramagnetic Resonance Absorption in Salts of the Iron Group, *Physical Review* **1947**, *72*(12), 1233-1240.

5. Gabrielse, G., Hanneke, D., Kinoshita, T., Nio, M., Odom, B., New Determination of the Fine Structure Constant from the Electron g Value and QED, *Physical Review Letters* **2006**, *97*, 030802.

6. Galli, C., Innes, J. B., Hirsch, D. J., Brudvig, G. W., Effects of Dipole-Dipole Interactions on Microwave Progressive Power Saturation of Radicals in Proteins, *J. Mag. Res., B.* **1996**, *110*, 284-287.

7. Hartree, D. R., Hartree, W., *Proc. R. Soc. London, Ser. A* **1948**, *193*, 299-304.

8. Kip, A. F., Kittel, C., Levy, R. A., Portis, A. M., Electronic Structure of F Centers: Hyperfine Interactions in Electron Spin Resonance, *Physical Review* **1953**, *91*, 1066-1071.

9. Morton, J. R., Preston, K. F., Atomic Parameters for Paramagnetic Resonance Data, *J. Mag. Reson*. **1978**, *30*, 577-582.

10. Scholes, C. P., Lapidot, A., Mascarenhas, R., Inubushi, T., Isaacson, R. A. and Feher, G., Electron Nuclear Double Resonance (ENDOR) from Heme and Histidine Nitrogens in Single Crystals of Aquometmyoglobin, *J. Am. Chem. Soc.* **1982**, *104,* 2724-2735.

11. Stoll, S., Schweiger, A., EasySpin, a comprehensive software package for spectral simulation and analysis in EPR, *J. Mag. Res.* **2006**, *178*, 42–55.

Introductory Books

1. Atherton, N.M., Principles of Electron Spin Resonance, New York: Ellis Horwood; Prentice Hall, **1993**.

2. Molecular Quantum Mechanics by Peter Atkins and Ronald Friedman. Chapter on magnetic properties of atoms and molecules, as well as a general understanding of a chapter on perturbation theory.

3. Magnetochemistry primer by A. F. Orchard. Chapter 2 and parts of Chapter 5.

4. NMR: The Toolkit primer by Peter Hore, Jonathan Jones and Stephen Wimperis.

5. Electron Paramagnetic Resonance primer by Victor Chechik, Emma Carter and Damien Murphy.

6. Barr, D. P., Eaton, G. R., Eaton, S. S., Weber, R. T, Quantitative EPR, Springer, **2010**.

7. Carrington, A., McLachlan, A. D., Introduction to Magnetic Resonance with Applications to Chemistry and Chemical Physics, New York, Harper & Row, **1967.**

8. Drago, R.S., Physical Methods for Chemists, Gainsville:Surfside, **1992**.

9. Weil, J. A., Bolton, J. R., Electron paramagnetic resonance: elementary theory and practical applications, New York; Chichester: Wiley, **2007**.

For ^{14}N, it follows that for an $I=1$ spin, the spin operators are

$$\hat{I}_x = \hbar \begin{bmatrix} 0 & 1/\sqrt{2} & 0 \\ 1/\sqrt{2} & 0 & 1/\sqrt{2} \\ 0 & 1/\sqrt{2} & 0 \end{bmatrix} \quad \hat{I}_y = \hbar \begin{bmatrix} 0 & -i/\sqrt{2} & 0 \\ 1/\sqrt{2} & 0 & -i/\sqrt{2} \\ 0 & 1/\sqrt{2} & 0 \end{bmatrix} \quad \hat{I}_z = \hbar \begin{bmatrix} 1 & 0 & 0 \\ 0 & 0 & 0 \\ 0 & 0 & -1 \end{bmatrix}$$

$$\hat{I}_+ = \hbar \begin{bmatrix} 0 & \sqrt{2} & 0 \\ 0 & 0 & \sqrt{2} \\ 0 & 0 & 0 \end{bmatrix} \qquad \hat{I}_- = \hbar \begin{bmatrix} 0 & 0 & 0 \\ \sqrt{2} & 0 & 0 \\ 0 & \sqrt{2} & 0 \end{bmatrix}$$

For ^{63}Cu and ^{65}Cu, it follows that for an $I=3/2$ spin, the spin matrices are

$$\hat{I}_x = \hbar \begin{bmatrix} 0 & \sqrt{3}/2 & 0 & 0 \\ \sqrt{3}/2 & 0 & 1 & 0 \\ 0 & 1 & 0 & \sqrt{3}/2 \\ 0 & 0 & \sqrt{3}/2 & 0 \end{bmatrix} \quad \hat{I}_y = \hbar \begin{bmatrix} 0 & -i\sqrt{3}/2 & 0 & 0 \\ i\sqrt{3}/2 & 0 & -i & 0 \\ 0 & i & 0 & -i\sqrt{3}/2 \\ 0 & 0 & i\sqrt{3}/2 & 0 \end{bmatrix}$$

$$\hat{I}_z = \hbar \begin{bmatrix} 3/2 & 0 & 0 & 0 \\ 0 & 1/2 & 0 & 0 \\ 0 & 0 & -1/2 & 0 \\ 0 & 0 & 0 & -3/2 \end{bmatrix} \quad \hat{I}_+ = \hbar \begin{bmatrix} 0 & \sqrt{3} & 0 & 0 \\ 0 & 0 & 2 & 0 \\ 0 & 0 & 0 & \sqrt{3} \\ 0 & 0 & 0 & 0 \end{bmatrix} \quad \hat{I}_- = \hbar \begin{bmatrix} 0 & 0 & 0 & 0 \\ \sqrt{3} & 0 & 0 & 0 \\ 0 & 2 & 0 & 0 \\ 0 & 0 & \sqrt{3} & 0 \end{bmatrix}$$

A.2a. Example calculation in Table 4. $\widehat{\mathcal{H}}_{SO} = \zeta \hat{L} \cdot \hat{S}$ operating on spin orbital $|d_{x^2-y^2},\alpha\rangle$ $\hbar = 1$

$$\widehat{\mathcal{H}}_{SO} = \zeta \hat{L} \cdot \hat{S} = \zeta[\hat{L}_x\hat{S}_x + \hat{L}_y\hat{S}_y + \hat{L}_z\hat{S}_z] = \zeta\left[\hat{L}_z\hat{S}_z + \left(\frac{\hat{L}_+ + \hat{L}_-}{2}\right)\left(\frac{\hat{S}_+ + \hat{S}_-}{2}\right) + \left(\frac{\hat{L}_+ - \hat{L}_-}{2i}\right)\left(\frac{\hat{S}_+ - \hat{S}_-}{2i}\right)\right]$$

$$= \zeta\left[\hat{L}_z\hat{S}_z + \frac{1}{4}(\hat{L}_+\hat{S}_+ + \hat{L}_-\hat{S}_+ + \hat{L}_+\hat{S}_- + \hat{L}_-\hat{S}_-) + \frac{1}{4i^2}(\hat{L}_+\hat{S}_+ - \hat{L}_-\hat{S}_+ - \hat{L}_+\hat{S}_- + \hat{L}_-\hat{S}_-)\right]$$

$$= \zeta\left[\hat{L}_z\hat{S}_z + \frac{1}{2}(\hat{L}_-\hat{S}_+ + \hat{L}_+\hat{S}_-)\right]$$

$$\widehat{\mathcal{H}}_{SO}|d_{x^2-y^2},\alpha\rangle = \zeta\left(\hat{L}_z\hat{S}_z + \frac{1}{2}(\hat{L}_-\hat{S}_+ + \hat{L}_+\hat{S}_-)\right)|d_{x^2-y^2},\alpha\rangle$$

$$= \zeta\left(\hat{L}_z\hat{S}_z + \frac{1}{2}(\hat{L}_-\hat{S}_+ + \hat{L}_+\hat{S}_-)\right)\left\{\frac{1}{\sqrt{2}}(|2,2\rangle + |2,-2\rangle)\right\}|\alpha\rangle$$

$$= \frac{\zeta}{\sqrt{2}}\left[\hat{L}_z\hat{S}_z|2,2\rangle|\alpha\rangle + \hat{L}_z\hat{S}_z|2,-2\rangle|\alpha\rangle + \frac{1}{2}\hat{L}_-\hat{S}_+|2,2\rangle|\alpha\rangle + \frac{1}{2}\hat{L}_-\hat{S}_+|2,-2\rangle|\alpha\rangle + \frac{1}{2}\hat{L}_+\hat{S}_-|2,2\rangle|\alpha\rangle\right.$$

$$\left. + \frac{1}{2}\hat{L}_+\hat{S}_-|2,-2\rangle|\alpha\rangle\right] \quad \leftarrow expand\ this\ yourself$$

$$= \frac{-\zeta}{\sqrt{2}}(|2,2\rangle - |2,-2\rangle)|\alpha\rangle + \frac{\zeta}{\sqrt{2}}(|2,-1\rangle)|\beta\rangle$$

$$Considering\ the\ following,$$

$$d_{xz} + id_{yz} = \frac{-1}{\sqrt{2}}(|2,1\rangle - |2,-1\rangle) - \frac{1}{\sqrt{2}}(|2,1\rangle + |2,-1\rangle) = \frac{-2}{\sqrt{2}}|2,1\rangle$$

$$d_{xz} - id_{yz} = \frac{2}{\sqrt{2}}|2,-1\rangle$$

$$conversion\ to\ Cartesian\ orbitals\ gives:$$

$$\widehat{\mathcal{H}}_{SO}|d_{x^2-y^2},\alpha\rangle = i\zeta|d_{xy},\alpha\rangle + \frac{\zeta}{2}|d_{xz},\beta\rangle + \frac{-i\zeta}{2}|d_{yz},\beta\rangle$$

A.2b. Expand wavefunction with Table 4. Given the copper spin-orbit coupling constant $\zeta = -830\text{cm}^{-1}$, use perturbation theory for first order corrections to the groundstate wavefunction $|d_{x^2-y^2},\alpha\rangle$ and $|d_{x^2-y^2},\beta\rangle$. The corrected wavefunction, $|a\rangle$, is related to the uncorrected wavefunction $|n\rangle$ by ($\hbar = 1$):

$$|a\rangle = |n\rangle - \sum_{m \neq n} \frac{\langle m|\hat{\mathcal{H}}_{SO}|n\rangle}{E_m - E_n}|m\rangle$$

$\hat{\mathcal{H}}_{SO}|d_{x^2-y^2},\alpha\rangle = \zeta \hat{L} \cdot \hat{S}|d_{x^2-y^2},\alpha\rangle$, using the two $d-d$ transitions of pg. $6-6$ & Table 4. Note -1*Δ b/c $E_m < E_n$.

$$|\Psi^+\rangle = |+\rangle = |d_{x^2-y^2},\alpha\rangle - i\frac{\zeta}{-\Delta_1}|d_{xy},\alpha\rangle + \frac{i}{2}\frac{\zeta}{-\Delta_2}|d_{yz},\beta\rangle - \frac{1}{2}\frac{\zeta}{-\Delta_2}|d_{xz},\beta\rangle$$

$$|\Psi^-\rangle = |-\rangle = |d_{x^2-y^2},\beta\rangle + i\frac{\zeta}{-\Delta_1}|d_{xy},\beta\rangle + \frac{i}{2}\frac{\zeta}{-\Delta_2}|d_{yz},\alpha\rangle + \frac{1}{2}\frac{\zeta}{-\Delta_2}|d_{xz},\alpha\rangle$$

A.2c. Electron Zeeman Hamiltonian with the prior wavefunction $\hat{\mathcal{H}}_{EZ} = \mu_B(\hat{L} + g_e\hat{S}) \cdot \vec{B}$

$$\hat{\mathcal{H}}_{EZ} = \mu_B(\hat{L}_x + g_e\hat{S}_x, \hat{L}_y + g_e\hat{S}_y, \hat{L}_z + g_e\hat{S}_z) \cdot (B_x, B_y, B_z)'$$

$$= \mu_B B_x(\hat{L}_x + g_e\hat{S}_x) + \mu_B B_y(\hat{L}_y + g_e\hat{S}_y) + \mu_B B_z(\hat{L}_z + g_e\hat{S}_z)$$

$(\hat{L}_z + g_e\hat{S}_z)|+\rangle = \hat{L}_z|d_{x^2-y^2},\alpha\rangle + i\frac{\zeta}{\Delta_1}\hat{L}_z|d_{xy},\alpha\rangle - \frac{i}{2}\frac{\zeta}{\Delta_2}\hat{L}_z|d_{yz},\beta\rangle + \frac{1}{2}\frac{\zeta}{\Delta_2}\hat{L}_z|d_{xz},\beta\rangle$ (use Table 2.)

$$+ g_e\hat{S}_z|d_{x^2-y^2},\alpha\rangle + i\frac{\zeta}{\Delta_1}g_e\hat{S}_z|d_{xy},\alpha\rangle + \frac{1}{2}\frac{\zeta}{\Delta_2}g_e\hat{S}_z|d_{xz},\beta\rangle - \frac{i}{2}\frac{\zeta}{\Delta_2}g_e\hat{S}_z|d_{yz},\beta\rangle$$

$$= 2i|d_{xy},\alpha\rangle + \frac{2\zeta}{\Delta_1}|d_{x^2-y^2},\alpha\rangle - \frac{\zeta}{2\Delta_2}|d_{xz},\beta\rangle + \frac{i\zeta}{2\Delta_2}|d_{yz},\beta\rangle$$

$$+ \frac{g_e}{2}|d_{x^2-y^2},\alpha\rangle + \frac{ig_e\zeta}{2\Delta_1}|d_{xy},\alpha\rangle - \frac{g_e\zeta}{4\Delta_2}|d_{xz},\beta\rangle + \frac{ig_e\zeta}{4\Delta_2}|d_{yz},\beta\rangle$$

$$= \left(2i + \frac{ig_e\zeta}{2\Delta_1}\right)|d_{xy},\alpha\rangle + \left(\frac{g_e}{2} + \frac{2\zeta}{\Delta_1}\right)|d_{x^2-y^2},\alpha\rangle - \frac{\zeta}{2\Delta_2}\left(1 + \frac{g_e}{2}\right)|d_{xz},\beta\rangle + \frac{i\zeta}{2\Delta_2}\left(1 + \frac{g_e}{2}\right)|d_{yz},\beta\rangle$$

$$\langle+|(\hat{L}_z + g_e\hat{S}_z)|+\rangle = \left\{\langle d_{x^2-y^2},\alpha| - \frac{i\zeta}{\Delta_1}\langle d_{xy},\alpha| + \frac{i\zeta}{2\Delta_2}\langle d_{yz},\beta| + \frac{\zeta}{2\Delta_2}\langle d_{xz},\beta|\right\}(\hat{L}_z + g_e\hat{S}_z)|+\rangle$$

$$= \frac{g_e}{2} + \frac{2\zeta}{\Delta_1} + \frac{2\zeta}{\Delta_1} + \frac{g_e\zeta^2}{2\Delta_1^2} - \frac{\zeta^2}{4\Delta_2^2}\left(1 + \frac{g_e}{2}\right) - \frac{\zeta^2}{4\Delta_2^2}\left(1 + \frac{g_e}{2}\right) \cong \frac{1}{2}\left(g_e + \frac{8\zeta}{\Delta_1}\right), noting \frac{g_e\zeta^2}{2\Delta_1^2} \sim 10^{-3}$$

Following $\langle-|(\hat{L}_z + g_e\hat{S}_z)|-\rangle, \langle-|(\hat{L}_x + g_e\hat{S}_x)|+\rangle, \langle+|(\hat{L}_x + g_x\hat{S}_x)|-\rangle, \langle-|(\hat{L}_y + g_e\hat{S}_y)|+\rangle, \& \langle+|(\hat{L}_y + g_e\hat{S}_y)|-\rangle$

Build the spin-Hamiltonian matrix:

	$|+\rangle$	$|-\rangle$
$\langle+|$	$\frac{\mu_B B_z}{2}\left(g_e + \frac{8\zeta}{\Delta_1}\right)$	$\frac{\mu_B B_x}{2}\left(g_e + \frac{2\zeta}{\Delta_2}\right) - \frac{i\mu_B B_y}{2}\left(g_e + \frac{2\zeta}{\Delta_2}\right)$
$\langle-|$	$\frac{\mu_B B_x}{2}\left(g_e + \frac{2\zeta}{\Delta_2}\right) + \frac{i\mu_B B_y}{2}\left(g_e + \frac{2\zeta}{\Delta_2}\right)$	$-\frac{\mu_B B_z}{2}\left(g_e + \frac{8\zeta}{\Delta_1}\right)$

Therefore, the coefficients of the magic pentagon are calculated for a strong tetragonal distortion in d^9.

$$g_\parallel = g_e + \frac{\mathbf{8\zeta}}{\Delta_1} \quad \& \quad g_\perp = g_e + \frac{\mathbf{2\zeta}}{\Delta_2}$$

Appendix B. CW-ESR Spectrometer Description

The microwave frequency operating range and design of CW-ESR spectrometers are based on adaptations of World War II radar technology and have evolved little since the 1970s. Nonetheless, in recent years the advent of inexpensive high-speed digitizers has facilitated innovation in CW-ESR, yielding improvements in signal to noise up to a factor of 10. Ensuing years of increased digitizer speeds and wide-band arbitrary wave-form generators in the GHz range will affect the future ESR instruments.

As shown in the Tuning Procedure page earlier, the basic formulation of a CW-ESR spectrometer involves a single, highly-stable microwave source that is power-leveled to exactly 200 mW and locked to the frequency of the resonator with an automatic frequency control (AFC) unit. The source microwaves split between two paths (1) the transmitter, circulator, and resonator, and (2) the reference. The two paths, or arms, meet in a coupling arm and are detected with a Schottky diode operating in a linear response regime: microwave power is rectified and given a low-pass filter to yield an output voltage that is proportional to the square root of the incident microwave power. In this sense the microwave circuit is called a bridge, in analogy to the electrical

measurements where a device under test generates a signal by affecting the balance of two large voltages, such as in resistance measurements of a Wheatstone bridge.
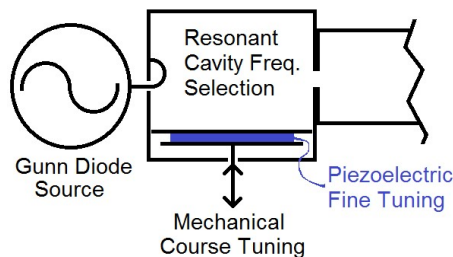
Scheme 2. The microwave source delivering a range of frequencies is coupled to a cavity that filters a single frequency. Frequency tuning is achieved with variation of the resonator dimension, with fine tuning achieved as an Automatic Frequency Control error voltage applied to a piezoelectric transducer.

One of the most important parts of the spectrometer for determining sensitivity is the microwave resonator, where microwave energy is stored prior to dissipation through resistive losses with the walls. As mentioned in the Signal Amplitudes section, a figure of merit for the resonator in CW-ESR is the Q-factor. The higher the Q-factor, the larger the number of cycles that microwave photons persist in the resonator and the higher the probability that they are absorbed by the sample. Likewise, a sample that completely fills the possible microwave magnetic field lines maximizes the filling factor, η, and the likelihood of absorption by the sample. The ESR resonator has an additional role of providing separation of the E-field and B-field components of the microwaves, providing a sample insertion volume of minimal E-field interaction.
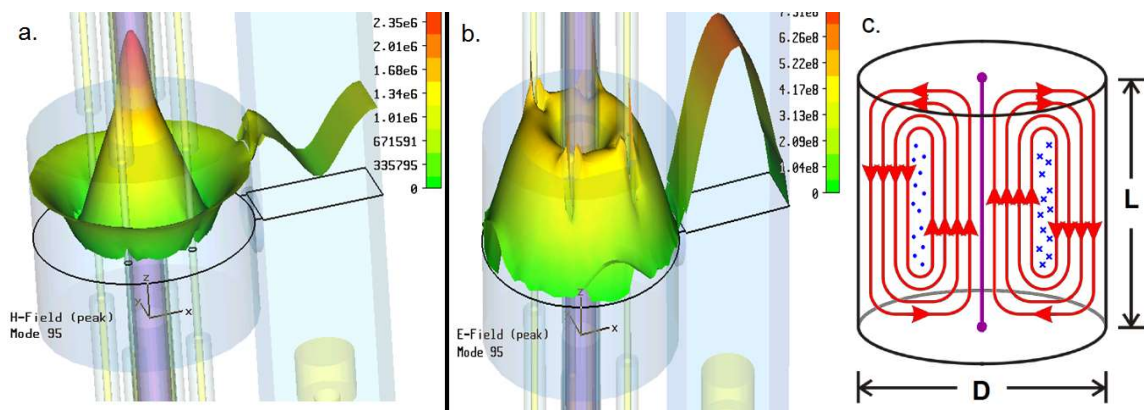
Figure 3. Calculated surface contours for the magnitude of H-field (panel a.) and E-field (panel b.) at the cross-section demarcated with the black line. The sample appears as a purple rod passing through the maximum of the H-field in the cylindrical resonator. A cross-section of the resonator field lines are in the panel c., where magnetic field lines are show in red, in the plane of the page, while the electric field lines are in blue as into and out-off the page, with the sample in purple. The resonator is attached through a side-wall coupling hole to the waveguide with a yellow tuning plunger visible in the bottom right. This resonator features internal modulation coils in a pseudo-Helmholtz arrangement. This is a TE_{011} mode cylindrical resonator (TE_{011}: Transverse Electric mode, cylindrical nodes are zero angular nodes, one radial node and one node in height), with an optimal Q-factor for dimensions L=D (=4cm for the Bruker resonator used in this practical).

Appendix C. A brief introduction to MATLAB and EasySpin

MATLAB is a general purpose scientific programming language, which is designed to be powerful and easy to use. EasySpin is a package of ESR simulation routines which runs using MATLAB. In order to use EasySpin, therefore, you will need to understand a little about MATLAB.

MATLAB syntax

This introductions starts with the very basics. These are, for the most part, very straightforward (but important) concepts. Try writing the examples in the MATLAB command window

1. Literals

Literals are values which appear written in the source code. For example the literal

    34

represents the number 34.

Numbers can also be written in exponential form. The literal

    6.626e-34

Represents the number 6.626×10^{-34}. The literal

    'perturb'

Represents a string of letters. Strings appear in purple in the MATLAB editor.

2. Comments

Comments are simply text in the code which is not part of the code. They appear in green in the MATLAB editor. They are preceded by a % symbol. For example

    % Set the value of a to 3
    a = 3;
    % The following line won't do anything
    % b = 6;

3. Variable Assignment

Variables are simply a way of referring to values. In maths, variables may have unknown values which are worked out later. In MATLAB, variables are assigned values based either on literals or on other variables. These values are assigned using =, e.g.

    a = 3
    b = 6
    c = a + b
    mu_b = 9.27400968e-24;
    hbar = 6.626e-34;

By default, MATLAB prints the results all assignments to the console. This tends to clutter up the view. Adding a semicolon after means that the output is not printed. If a value is written, but not assigned to anything, the value gets assigned to the temporary variable ans.

4. Vectors and matrices

Vectors and *matrices* are written using square brackets, e.g.

    g = [2.05, 2.05, 2.1];

defines a 3x1 row vector. Use semicolons to write column vectors

```
    r = [1; 4; 2];
```
There's also a quick notation to assign a row variable in one go. The code
```
    x = 1:5;
```
sets x equal to [1, 2, 3, 4, 5]. This notation is particularly useful for loops.

5. Structures

Structures are simply collections of variables. Collecting the variables into a structure allows for logical organisation of variables into groups, and makes it easier to pass a set of related variables to a function. Structures have *fields*, which are simply the names of the variables collected in the structure. In MATLAB, these fields are *referenced* using the '.' operator.

For example, the lines
```
    sys.S = 1/2;
    sys.g = 2.0023;
    sys.lwpp =0.5;
```
defines a structure called sys, with fields S, g and lwpp. The structure collects together information about a spin system. EasySpin uses this information to perform the simulation. EasySpin makes extensive use of structs.

6. Functions

Functions take a number of parameters, perform some kind of operation on them, and return some number of parameters as a result.

For example, the function sqrt:
```
    b = sqrt(a);
```
takes the square root of the variable a and returns the value, which is then assigned to the variable b.

7. Indexing

Indexing means referring to a particular value (or set of values) in a matrix or vector. Indexing uses *subscripts*, which are written in brackets after the variable name. For an example, consider the following:
```
    x = [1, 2, 3, 4, 5]
    y = x(5)            % y is now equal to 5
    x(3) = -10          % x now equals [1, 2, -10, 4, 5]
```
The first element of a vector is element 1. The last can be referred to by using 'end'.
```
    x =[1, 2, 3]
    x(end) = 7                 % x now equals [1, 2, 7]
    x(end-1) = 4        % x now equals [1, 4, 7]
    x(end+1) = 6        % x now equals [1, 4, 7, 6].
```
In a matrix, you can refer to whole rows or columns by using the ':' operator
```
    x = magic(5)        % creates a 5x5 magic square matrix
    x(:,3) = 0          % sets the 3rd column of x equal to zero
    x(2,:) = 7          % sets the 2nd row of x equal to 7
```

8. Loops

Loops cause the same piece of code to run repeatedly. The number of times the code runs is determined by the *loop variable*. It's easiest to show by example

```
x = [1,3,7,3]
for k = 1:length(x)
    y(k) = x + k
end
% y now equals [2, 5, 10, 7]
```

This code sets the variable x. It then iterates over the variable k. It first sets the value of k to the value of the first element in the vector [1, 2, 3 ... n], where n is the number of items in x. It then executes the code between the for and end lines, which in this case sets the value of the k-th element of y. Finally, the code returns to the top. It sets k to the next value in the vector [1, 2, 3 ... n], and the process completes. The loop ends when the loop has been run with k equal to all values in the vector.

Selected EasySpin functions and structure fields:

Spin System Structure
This is generally called sys
        sys.g = [a, b, c];
Sets the g-tensor of the electron being simulated.
If a = b= c, the g-tensor is isotropic.
If a = b ≠ c, the g-tensor is axial
If a ≠ b ≠ c, the g-tensor is orthorhombic
        sys.lwpp = x;
Sets the peak-to-peak line-width of peaks in the simulation, in mT.
        sys.Nucs = '63Cu';
        sys.Nucs = 'Cu';
        sys.Nucs = '63Cu,14N,14N';
Sets the nuclei present in the system.
'63Cu' performs a simulation using a ^{63}Cu nucleus. 'Cu' performs the simulation assuming that the different isotopes of copper are present in their natural abundances. Extra nuclei are added in a comma-separated list.
        sys.A = [-100, -100, -630];
        sys.A = [-100, -100, -630; 54, 45, 45; 54, 45, 45;];
Sets the hyperfine coupling (A-tensor) in MHz. Each row consists of 3 columns, with the principal values of the tensor, and corresponds to a nucleus defined in the Nucs field.
        sys.logtcorr = -4
Sets the rotational correlation time, τ_r, of the system, such that $\log_{10} \tau_r$ is equal to the sys.logtcorr.

Experimental Parameters Structure
This is generally called exp
        exp.mwFreq = 94;
        exp.mwFreq = 9.5;
The operating frequency of the spectrometer, in GHz. X-band is 9.5 GHz, W-band is 94 GHz.
        exp.Range = [300, 325]
The magnetic field range (in mT) over which to perform the simulation. If this option is not set, then EasySpin sets the range automatically. Unfortunately, this automatic setting sometimes fails to work. In this case the range must be set using this command.

exp.Orientations

Sets the single-crystal orientations to be simulated. If this field is not set, or is empty, then the powder average (or frozen solution average) over all orientations is calculated.

Setting exp.orientations can be a little tricky; see at the bottom for a hint.

Options Structure

This is generally called opt

opt.Method = 'perturb'

Sets the calculation method to be based on 2nd-order perturbation theory. This is much faster than the default method.

opt.Output = 'separate'

Causes EasySpin outputs one row for each spectrum, corresponding to a row in the 'exp.Orientations' variable.

opt.nKnots = 901

Increases the number of orientations over which powder (or frozen solution) averages are performed. More knots take more time to calculate, but give a better answer. 901 knots is usually excessive, but doesn't take too long to compute for the straightforward systems we're considering.

Functions:

pepper(sys, exp, opt)

[B, spec] = pepper(sys, exp, opt);

Calculates solid-state spectra. In the first case, pepper automatically plots the spectrum. In the second case, the field values are saved to B, and the spectrum to spec.

chili(Sys,Exp);

Calculates the slow-motional spectrum, using a correlation time set by sys.logtcorr

stackplot(B, spec)

produces a stacked plot, where each trace corresponds to one row of spec.

More information on these can be found in the EasySpin *help files*.

How to set the exp.Orientations matrix

To perform a simulation over a range of orientations, we must supply an orientations matrix. This is a 3 x n matrix. If a row of the matrix is of the form [0, x, 0], then it represents a rotation of the z-axis. [0, 0, 0] represents a crystal with z-axis aligned parallel to B, [0, pi/2, 0] represents a crystal with z-axis aligned perpendicular to B.

While we could just perform a loop over all orientations, this is quite slow. It is far faster to calculate all orientations at once. To do that we need to make an orientations matrix.

The first step is to define what orientations we want to test:

n = 31;

OrientationsToTest = linspace(0, pi/2, n);

This command creates a vector with n elements, equally spaced between 0 and pi/2.

Next, we create a matrix to hold the orientation values. We make sure it's of the correct size, containing only zeros:

exp.orientations = zeros(3,n);

Finally, we replace the middle column with the orientations we made above.

exp.orientations(2,:) = OrientationsToTest.';

Note the .' after OrientationsToTest. This tells MATLAB to take the transpose of the row vector, OrientationsToTest. This converts it into a column vector, which we assign to the middle column of orientations.

So, in the end, the code is:

n = 31;

OrientationsToTest = linspace(0, pi/2, n);

exp.orientations = zeros(3,n);

exp.orientations(2,:) = OrientationsToTest.';

Bonus Hint

It's possible to define short (one-line) functions as follows:

a = @(x,y) x + y

Then call the function as follows

b = a(3,2) % b = 5

This can be useful, e.g.:

```
h = 6.626e-34;          % in J s
mu_b = 9.274e-24;       % in J per T
g_to_B = @(freq, g) h * (freq * 1e9) ./ (mu_b * g) * 1e3;
% The factor of 1e9 converts GHz to Hz
% The factor of 1e-3 converts T to mT
B = g_to_b(9.5, 2.02)
```

This converts a g-value to a field strength (in mT) using a spectrometer frequency (in GHz). A similar function can be defined to convert field strengths to g-values.

Code for making plots.

```matlab
% This function saves the current Figure in PNG format.
% file - is appended with '.png'
% dpi - is dots per inch, recommended 400
% w_inch - is width in inches

function [] = esrProof(file,dpi,w_inch)
scsize=get(0,'ScreenSize');
ppi=get(0,'ScreenPixelsPerInch');
sizexw=w_inch*ppi;
ratio=scsize(4)/scsize(3);
sizeyh=round(ratio*sizexw);
pos1=[1,31,sizexw,sizeyh];
pr_res=strcat('-r',num2str(dpi));
print ('-dpng',pr_res,file);
end

===============================================

% Example plotting code for a stack plot,
% with offsets having already been applied to data arrays
% subplot – see Matlab help file.

subplot(1,1,1)
plot(x1,Yo1,'r',x2,Yo2,'b',x3,Yo3,'k','LineWidth',1);
axis tight; pbaspect([1 1.5 1]);
ylim([1.05*min(min([Yo1 Yo2 Yo3])) 1.05*max(max([Yo1 Yo2 Yo3]))]);
xlabel('B_0 (mT)','FontName','Arial','FontSize',10);
ylabel('d\chi"/dB','FontName','Arial','FontSize',10);
title('Hyperfine Splittings of CuTPP m_I=3/2 peak','FontName','Arial','FontSize',10);
l=legend('^{63}Cu','^{65}Cu','Nat. Abnd. Cu');
set(gca,'ytick',[],'LineWidth',1,'FontName','Arial','FontSize',10);
set(l,'Location','Northeast','FontName','Arial','FontSize',8);

esrProof('SimulationExercise_04',400,4);

===============================================

% Example plotting code for an intensity surface
% pcolor – see Matlab help file.

pcolor(x',orients',Ys');  %sizes are x(m),y(n),& z(m x n)
shading flat;
axis tight; pbaspect([2 1 1]);
% xlim([-0.01 0.01]+mean(sys.g));
xlabel('B_0 (mT)','FontName','Arial','FontSize',12);
ylabel('d\chi"/dB','FontName','Arial','FontSize',12);
title('Single Xtal Orients, \Delta\theta=0.1 deg.','FontName','Arial','FontSize',12);
set(gca,'ytick',[],'LineWidth',1.0,'FontName','Arial','FontSize',12) ;
```